DOI: 10.1002/chem.200500921

Novel 2,1,3-Benzothiadiazole-Based Red-Fluorescent Dyes with Enhanced Two-Photon Absorption Cross-Sections

Shin-ichiro Kato,[a] Taisuke Matsumoto,[b] Motoyuki Shigeiwa,[c] Hideki Gorohmaru,[c] Shuuichi Maeda,[c] Tsutomu Ishi-i,[b] and Shuntaro Mataka*[b]

Abstract: This paper reports the two-photon absorbing and orange-red fluorescence emitting properties of a series of new 2,1,3-benzothiadiazole (BTD)-based D–π–A–π–D-type and star-burst-type fluorescent dyes. In the D–π–A–π–D-type dyes **1**–**6**, a central BTD core was connected with two terminal *N*,*N*-disubstituted amino groups via various π-conjugated spacers. The star-burst-type dyes **8** and **10** have a three-branched structure composed of a central core (benzene core in **8** and triphenylamine core in **10**) and three triphenylamine-containing BTD branches. All the BTD-based dyes displayed intense orange-red color fluorescence in a region of 550–689 nm, which was obtained by single-photon excitation with good fluorescent quantum yield up to 0.98 as well as by two-photon excitation. Large two-photon absorption (TPA) cross-sections (110–800 GM) of these BTD dyes were evaluated by open aperture *Z*-scan technique with a femtosecond Ti/sapphire laser. The TPA cross-sections of D–π–A–π–D-type dyes **2**–**6** with a benzene, thiophene, ethene, ethyne, and styrene moiety, respectively, as an additional π-conjugated spacer are about 1.5–2.5 times larger than that of **1c** with only a benzene spacer. The TPA cross-sections significantly increased in three-branched star-burst-type BTDs **8** (780 GM) with a benzene core and **10** (800 GM) with a triphenylamine core, which are about 3–5 times larger than those of the corresponding one-dimensional sub-units **9** (170 GM) and **11** (230 GM), respectively. The ratios of σ/e_{π} between three-branched and one-dimensional dyes were 6.5:3.8 (for **8** and **9**) and 6.0:4.0 (for **10** and **11**), which are larger than those predicted simply on the basis of the chromophore number density (1:1), according to a cooperative enhancement of the two-photon absorbing nature in the three-branched system.

Keywords: donor–acceptor systems · fluorescence · two-photon absorption

Introduction

Organic molecules exhibiting significant nonlinear optical nature have been the subject of various scientific studies in recent years. In particular, highly active two-photon absorbing molecules have attracted considerable attention in the last decade, although two-photon absorption (TPA) was predicted theoretically by Göppert-Mayer in 1931.[1] Photoexcitation as well as frequency-upconverted fluorescence of molecules on the TPA process are confined to the focal point, since the probability of TPA is proportional to the square of the light intensity. These features produced potential applications for optical power limitation,[2] microfabrication,[3] three-dimensional optical data storage,[4] photodynamic therapy,[5] and two-photon laser scanning fluorescence imaging.[6] Among these applications, two-photon laser scanning fluorescence imaging that uses near IR photons as the excitation source has gained widespread popularity in the biological community, which provides images at an increased penetration depth in tissue with less photodamage. Recently, much progress has been made in two-photon laser scanning fluorescence imaging by using two-photon confocal laser scanning microscopy,[7] which has promoted synthetic studies to develop TPA fluorophore for biomolecular tags.[8] There-

[a] S.-i. Kato
Interdisciplinary Graduate School of Engineering Sciences
Kyushu University, 6-1 Kasuga-koh-en
Kasuga 816-8580 (Japan)

[b] T. Matsumoto, Dr. T. Ishi-i, Prof. Dr. S. Mataka
Institute for Materials Chemistry and Engineering (IMCE)
Kyushu University, 6-1 Kasuga-koh-en
Kasuga 816-8580 (Japan)
Fax: (+81) 92-583-7894
E-mail: mataka@cm.kyushu-u.ac.jp

[c] M. Shigeiwa, Dr. H. Gorohmaru, Dr. S. Maeda
Mitsubishi Chemical Group Science
and Technology Research Center, Inc.
1000 Kamoshida-cho, Aoba-ku, Yokohama 227-8502 (Japan)

fore, it is important to understand the nature of the relationship between the molecular structure and the TPA property to provide guidelines for the development of materials with large TPA cross-sections at the wavelength of available laser sources. Brédas, Marder, Perry, and Webb's group designed bis(styryl)benzene derivatives with electron donor (D), electron acceptor (A), and π-spacer (π), and achieved large TPA cross-sections on the basis of a concept that the TPA nature is ascribed to intramolecular charge transfer (ICT).[9] Subsequently, a number of compounds including D–A–D-type molecules,[10,11] D–π–A-type molecules,[12–15] A–D–A-type molecules,[16–18] D–π–D-type molecules,[19–21] macrocycles,[22–24] multi-branched molecules,[25–30] and organometallic complexes[31] were synthesized, and their TPA properties were investigated. Then, it has been pointed out that expansion of π-electron conjugation is crucial for large TPA cross-sections. In addition, a significant increase in the TPA ability has been discovered in the multi-branched structures, indicating a cooperative enhancement.[25a,c,g,27b,c,30]

The fluorescent color emitted from TPA dyes has mostly been restricted to blue and green; nevertheless various types of compounds exhibiting large TPA cross-sections are now accessible as described above. The blue and green colors would interfere with the self-absorption wavelength of the cell. In order to achieve efficient two-photon laser scanning fluorescence imaging, two-photon absorbing fluorophores are required to emit fluorescence in the red region. However, strong red emission with two-photon excitation is scarce compared with the two colors mentioned above, because an elongated π-system in the two-photon absorbing fluorophores is required to obtain red-emission by direct two-photon excitation.[32] Therefore, more effort is needed to achieve promising red-fluorescent TPA materials. Fréchet and Prasad's group designed bichromophoric molecules with the TPA chromophore and the red-fluorescence emitting moiety, which can avoid the difficulty of adding a red-emission property to TPA dyes, and achieved intense red-color emission indirectly by efficient intramolecular fluorescent resonance energy transfer.[32a,b] Recently, we reported the first example of red-fluorescent TPA dyes by direct two-photon excitation using 2,1,3-benzothiadiazole (BTD)-based fluorescent dyes.[33] At almost the same time, Müllen and his co-workers synthesized water-soluble and red-fluorescent perylene diimides,[32c] which can be developed to living cell imaging by direct two-photon excitation by Hofkens and Schryver's group.[32d] More recently, an excellent

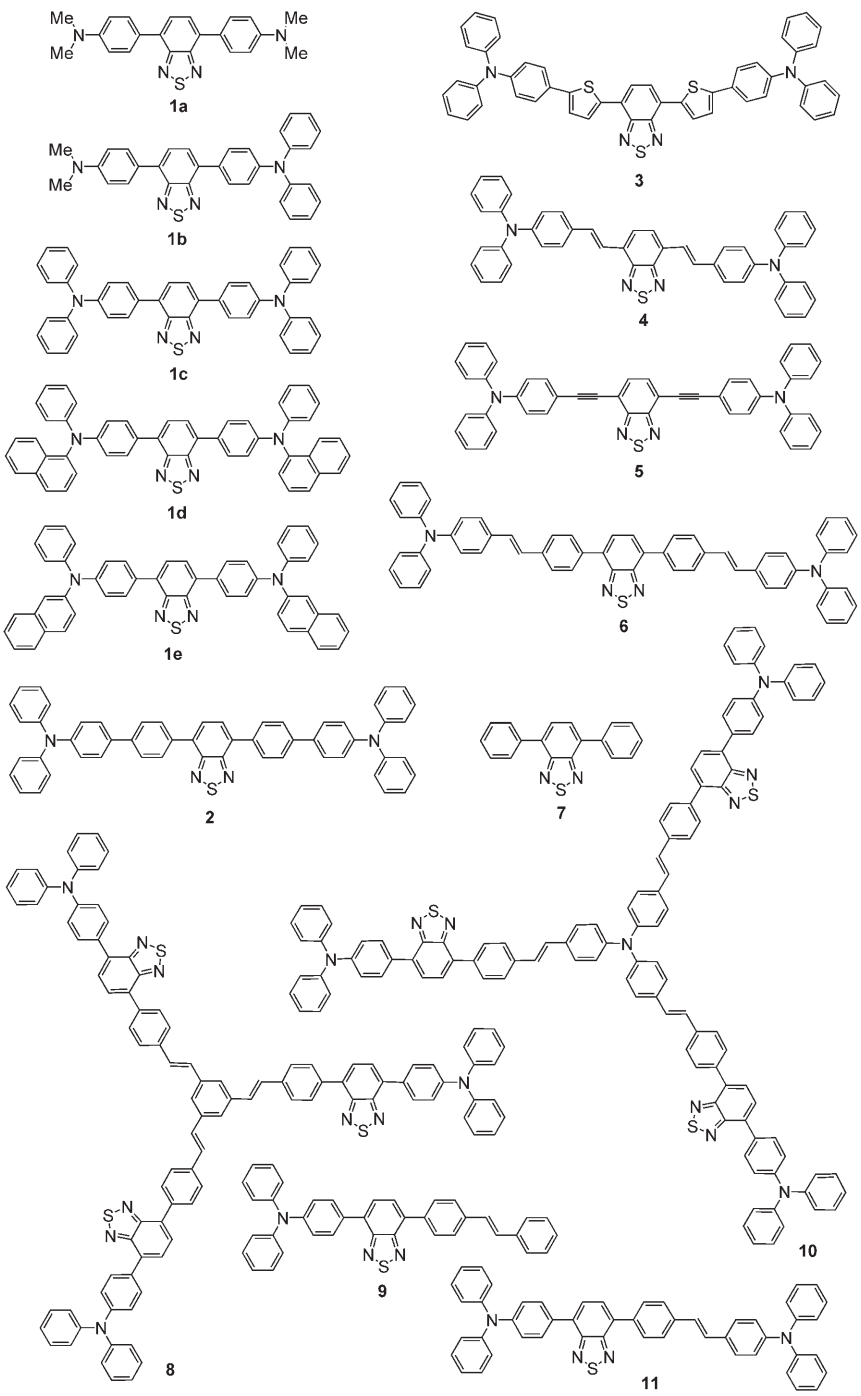

TPA dye of Eu^{III} complex with high purity red emission was created by Zhang and Wang group.[32e] The structures of D–π–A–π–D-type and star-burst-type 2,1,3-benzothiadiazoles **1**–**11** are depicted below.

4,7-Diphenyl-2,1,3-benzothiadiazole and its derivatives are known to be strongly fluorescent dyes, which exhibit large Stokes shifts.[34,35] Furthermore, an electron-withdrawing 2,1,3-benzothiadiazole (BTD) unit was used as an important spacer in semiconducting oligomers.[36] Recently, we have developed BTD-based dyes to functional materials such as dichroic fluorescent materials in liquid crystal displays,[37] and a light-harvesting antenna as well as an energy-transfer reagent in a fullerene-dyad system.[38] We expected that a strong red emission by direct two-photon excitation would be achieved by using the strong fluorescent and electron-accepting nature of the BTD dye. BTD-based TPA dyes, so-called donor–π-bridge–acceptor–π-bridge–donor (D–π–A–π–D)-type dyes, were designed and prepared on the basis of a combination of the BTD moiety and two terminal electron-donating amino groups by π-conjugated spacers to enhance the ICT character.[33] As a part of our continuing work to develop BTDs as red-fluorescent TPA materials, we report here the detailed results of six kinds of D–π–A–π–D-type dyes **1**–**6** (see above) with different π-conjugate length. The TPA ability is discussed on the basis of absorption and fluorescent solvatochromism, X-ray crystallographic analysis, as well as *Z*-scan TPA cross-section measurement, whereas their red-fluorescent nature is discussed based on single- and two-photon excited fluorescence spectroscopy. In addition, two kinds of BTD-based star-burst-type derivatives **8** and **10** have been synthesized to enhance TPA ability by a cooperative effect. Significantly large TPA cross-section up to 800 GM is achieved in the start-burst structures together with the attractive red-fluorescence. Finally, correlation between the two parameters "TPA cross-section and fluorescent quantum yield" is discussed to characterize molecular ability for the development to the two-photon laser scanning fluorescence imaging.

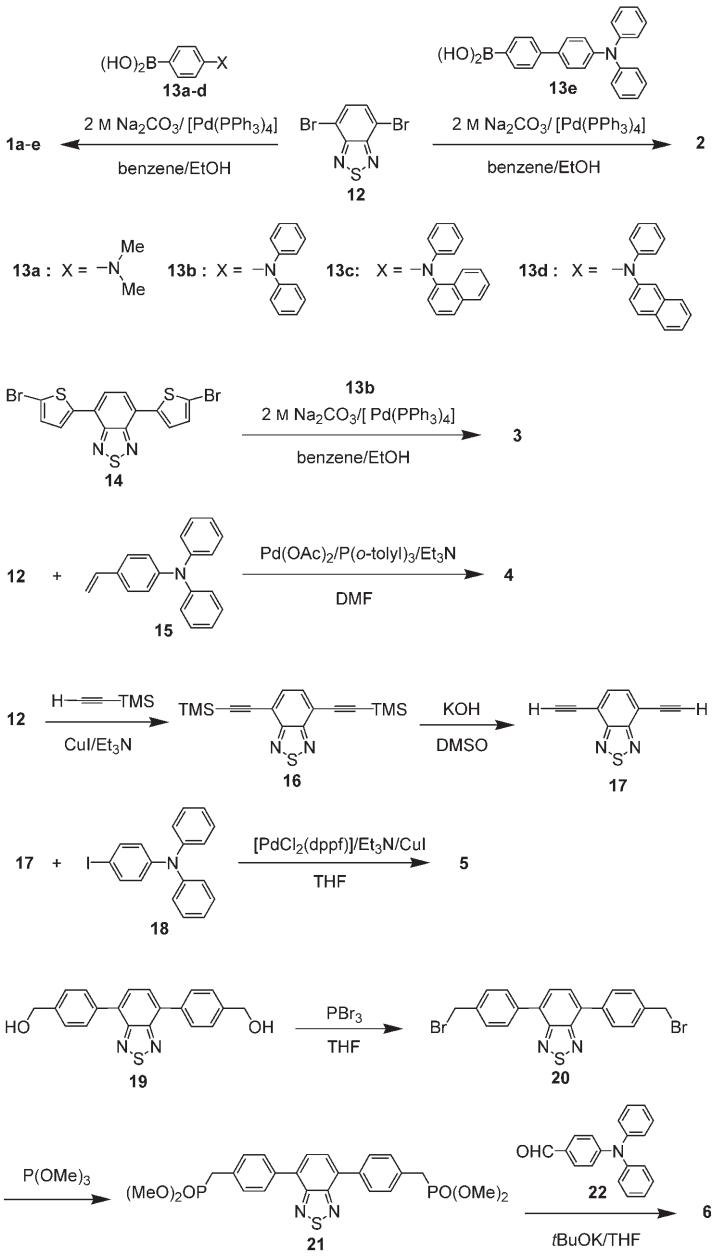

Scheme 1. Preparation of D–π–A–π–D-type 2,1,3-benzothiadiazoles **1**–**6**.

Results and Discussion

Synthesis: The synthesis of D–π–A–π–D-type BTDs **1**–**6** was achieved by means of palladium-mediated cross-coupling reactions of 4,7-dibromo-2,1,3-benzothiadiazole (**12**) as shown in Scheme 1. To observe the influence on the photophysical properties of the substituents such as methyl, phenyl, and naphthyl groups on the nitrogen atom, **1a**–**e** with various *N*,*N*-disubstituted amino groups with only benzene spacers between the BTD moiety and the amino nitrogen atoms were synthesized by Suzuki coupling reactions of **12** with the corresponding arylboronic acids **13a**–**d** in 50–70% yields in the presence of a palladium(0) catalyst. To enhance π-conjugation relative to **1c**, other BTD derivatives **2**–**6** having a benzene, thiophene, ethene, ethyne, and styrene moiety, respectively, as an additional spacer between the BTD ring and the amino group were prepared. Compound **2** with the additional benzene ring was prepared by Suzuki coupling reaction of **12** with 4′-(*N*,*N*-diphenylamino)-biphenyl-4-yl-boronic acid (**13e**) in 18% yield according to the procedure described above. Similarly, **3** with the thiophene ring was obtained by a Suzuki coupling reaction of 4,7-bis(5-bromo-2-thienyl)-2,1,3-benzothiadiazole (**14**) with **13b** in 33% yield. The introduction of the additional ethene spacer in **4** was performed by Heck reaction of **12** with 1-(*N*,*N*-diphenylamino)-4-vinylbenzene (**15**) catalyzed by palladium acetate/tris(*o*-tolyl)phosphine in the presence of triethylamine in 17% yield. Sonogashira coupling reaction of 4,7-diethynyl-2,1,3-benzothiadiazole (**17**) with 4-(*N*,*N*-diphenylamino)iodobenzene (**18**) gave **5** with the additional ethyne spacer in 11% yield. The synthetic intermediate **17**

was derived from **12** by coupling reaction with trimethylsilylacetylene followed by treatment with potassium hydroxide. BTD **6** with the additional styrene spacer was obtained from the bishydroxymethyl derivative **19** in three steps. Bromination of **19** by phosphorus tribromide afforded the dibromide **20** in 44% yield, which was converted to the diphosphate **21** by treatment with trimethyl phosphite in high yield. Finally, double Horner–Emmons reaction of **21** with triphenylamine aldehyde **22** in the presence of potassium *tert*-butoxide afforded the desired **6** in 61% yield.

To enhance the TPA ability, three-branched star-burst-type BTDs **8** and **10** were designed and prepared as shown in Scheme 2. The star-burst-type BTD **8** with a benzene core was obtained from monoaldehyde of BTD **23** and triphosphate **27** under triple Horner–Emmons reaction conditions in 63% yield. Similarly, another star-burst-type BTD **10** with a triphenylamine core was obtained from monophosphate of BTD **26** and trialdehyde **29** under Horner–Emmons reaction conditions in 59% yield. The key synthetic intermediate **26** was derived from **23** in three steps (reduction, bromination, and phosphorylation) according to a similar procedure in the synthesis of **6**. One-dimensional BTD-based dye **9** was obtained by Wittig reaction of **23** as reference of **8** with the benzene core. Similarly, **11** was prepared as reference of **10** with the triphenylamine core. All new dyes have been fully characterized by spectroscopy and elemental analysis.

Single-photon absorption and emission properties: The single-photon excited absorption and fluorescence properties of D–π–A–π–D-type BTDs **1**–**6** are summarized in Table 1; the data of star-burst-type BTDs **8** and **10** are shown in Table 2 along with their references **9** and **11**. The single-photon absorption (SPA) and single-photon excited fluorescence (SPEF) spectra were measured in toluene and dichloromethane to investigate the influence of solvent polarity on optical properties of BTDs. The SPA spectra of BTDs have two bands around 300–380 and 420–550 nm arising from π–π* and charge-transfer transitions, respectively.[35] The SPA maxima (λ_{max}) of all the BTDs were scarcely changed between nonpolar toluene and polar dichloromethane (Tables 1 and 2). In the D–π–A–π–D-type BTDs **1a**–**e**, the absorption coefficients (ε) depended on the substituents on the nitrogen atom (13000–21400). Compared with **1c** with only a benzene spacer (19500–20500), **3**–**6** with the expanded π-spacer largely increased the ε values (32300–49300), except for **2** (22300–23200) (Figure 1 and Table 1). More significant enhancement of the ε values was observed in three-branched star-burst-type BTDs **8** (70000–71400) and **10** (115400–115900). The ε values of **8** and **10** were about 3.5 times larger than those of the one-dimensional sub-units **9** and **11**, respectively (Figure 2 and Table 2). The multidimensionality in the star-burst systems **8** and **10** leads the increase of oscillator strength.

All the BTD derivatives emitted orange-red fluorescence at the wavelength region of 550–689 nm and exhibited significant solvatochromism contrary to the absorption process. With increasing solvent polarity, the SPEF maxima (λ_{SPEF}) showed remarkable bathochromic shifts. As a typical example of this phenomenon, the SPEF spectra of D–π–A–π–D-type BTD **4** and star-burst-type BTD **10** are shown in Figure 3, which provide the differences of λ_{SPEF} between toluene and dichloromethane of 66 nm in **4** and 55 nm in **10**. Furthermore, the fluorescent quantum yields (φ_f) in dichloromethane solution of all the BTDs were smaller than those in toluene solution (Table 1). Considerably high φ_f values of all the BTDs are maintained in toluene solution among the orange-red color region. In order to examine in detail the solvent effect, the SPEF spectra of **1c** were measured in various media from nonpolar to polar solvents. With increasing solvent polarity from cyclohexane, toluene, THF, dichloromethane, PhCN, to DMF, the λ_{SPEF} values of **1c** shifted significantly to longer wavelength region by 100 nm (from 557 nm in cyclohexane, to 657 nm in DMF) along with

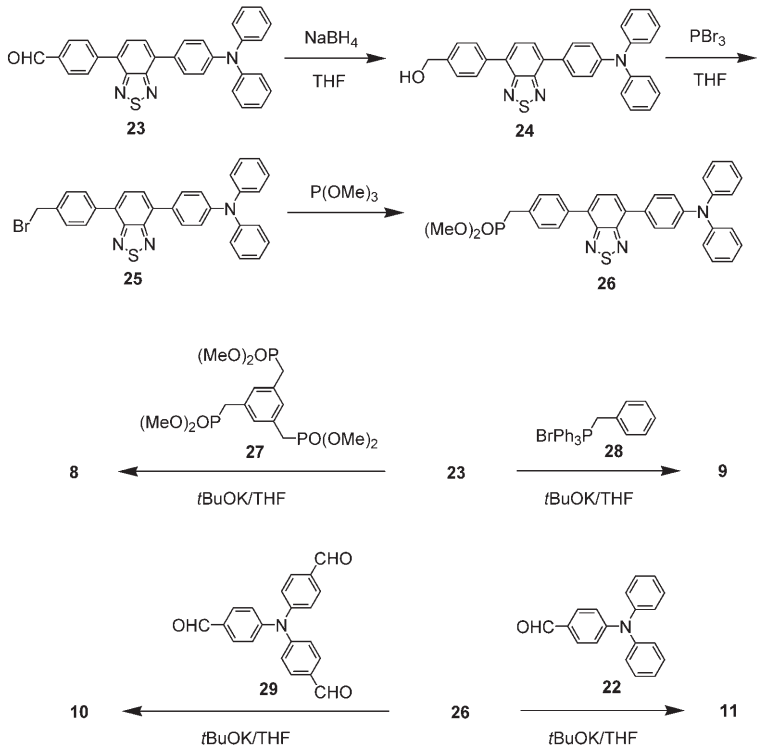

Scheme 2. Preparation of star-burst-type 2,1,3-benzothiadiazoles **8**–**11**.

Table 1. Single- and two-photon properties of D–π–A–π–D-type 2,1,3-benzothiadiazoles **1**–**6**.

	λ_{max}/nm ($10^{-2}\varepsilon$)[a]		λ_{SPEF}/nm[b] (φ_f)		$\varphi_f\times\varepsilon$[c]	$\varphi_f\times\sigma$[c] /GM	λ_{TPEF}[f] /nm	σ/GM[g] /nm
	Toluene	CH_2Cl_2	Toluene	CH_2Cl_2				
1a	472	473	624	680	6070	51	628	120[h]
	(148)	(130)	(0.41[c])	(0.13[c])	(1690)	(16)		(760)
1b	468	464	612	660	8600	59	614	120[h]
	(172)	(156)	(0.50[c])	(0.23[c])	(3590)	(27)		(780)
1c	462	458	592	640	12700	83	599	130[h]
	(205)	(195)	(0.62[c])	(0.36[c])	(7020)	(48)		(780)
1d	462	458	588	634	13000	74	599	120[h]
	(203)	(190)	(0.64[c])	(0.52[c])	(9880)	(60)		(780)
1e	465	461	591	646	13700	71	599	110[i]
	(214)	(210)	(0.64[c])	(0.40[c])	(8400)	(44)		(780)
2	426	422	550	657	22700	190	552	200[j]
	(232)	(223)	(0.98[d])	(0.14[d])	(3120)	(27)		(780)
3	530	529	661	689	18100	160	670	280[k]
	(323)	(364)	(0.56[c])	(0.15[c])	(5460)	(42)		(780)
4	512	511	617	683	27100	220	642	330[l]
	(417)	(416)	(0.65[c])	(0.23[c])	(9570)	(77)		(780)
5	480	484	568	663	31000	160	586	200[l]
	(392)	(380)	(0.79[c])	(0.19[c])	(7220)	(38)		(780)
6	443	437	564	654	30900	210	569	330[m]
	(490)	(493)	(0.63[c])	(0.05[c])	(2470)	(17)		(780)

[a] Measured in a 1×10^{-5} M solution. [b] Measured in a 1×10^{-6} M solution. [c] Fluorescent quantum yield relative to rhodamine B in ethanol (0.65). [d] Fluorescent quantum yield relative to fluorescein in ethanol (0.97). [e] In toluene solution, whereas the value in parentheses is in dichloromethane solution. [f] $\lambda_{ex}=800$ nm in toluene solution. [g] The maximal TPA cross-sections (σ) in toluene were estimated by using AF-50 (61 GM at 780 nm) (3.3×10^{-3} M) as a reference. The value in parentheses is absorption wavelength. 1 GM (Göppert–Mayer) $=1\times10^{-50}$ cm^4s per photon per molecule. [h] Measured in a 5×10^{-3} M toluene solution. [i] Measured in a 1×10^{-3} M toluene solution. [j] Measured in a 3.7×10^{-3} M toluene solution. [k] Measured in a 0.94×10^{-3} M toluene solution. [l] Measured in a 2.0×10^{-3} M toluene solution. [m] Measured in a 1.6×10^{-3} M toluene solution.

groups and **1b** with one dimethylamino group have smaller φ_f values (0.13 in **1a** and 0.23 in **1b**) in dichloromethane. In **2**–**6**, the additional spacer between the BTD ring and the amino groups tends to decrease the φ_f values. For example, the φ_f value (0.23) of **4** with the additional ethene spacer in dichloromethane solution is almost two-thirds of that (0.36) of **1c** with only the benzene spacer (Table 1). In star-burst-type BTDs, the φ_f value (0.07 in dichloromethane) of **10** with a triphenylamine core is significantly lower than that (0.39 in dichloromethane) of **8** with a benzene core. In spite of this disadvantage, **10** is still a good emitter, because the ε value of **10** is quite large (115400) compared with other BTD derivatives without star-burst structure. A parameter of $\varepsilon\times\varphi_f$ (8080 in dichloromethane) in **10** was higher than that (2470) of **6**

decreasing the fluorescence intensity (Figure 4 and Table 3). The fluorescent quantum yields (φ_f) from 0.85 in cyclohexane to 0.22 in DMF were reduced indeed with increasing the solvent polarity (Table 3). On the other hand, the SPA maxima (λ_{max}) of **1c** were independent of the solvent polarity (Table 3). These results indicate that the structure of the excited state (assumed to be the first excited state S_1) in BTD dyes is more polar than that of the ground state. One can conclude that in the BTD dyes the ICT actually occurs between the terminal amino group and the BTD ring.

Table 2. Single- and two-photon properties of star-burst-type 2,1,3-benzothiadiazoles **8**–**11**.

Compd	λ_{max}/nm ($10^{-2}\varepsilon$)[a]		λ_{SPEF}/nm[b] (φ_f)[c]		$\varphi_f\times\varepsilon$[d]	$\varphi_f\times\sigma$[d] /GM	λ_{TPEF}[e] /nm	σ/GM[f] /nm	σ/e_π
	Toluene	CH_2Cl_2	Toluene	CH_2Cl_2					
8	451	446	577	636	50400	560	591	780[g]	6.5
	(700)	(714)	(0.72)	(0.39)	(27800)	(310)		(720)	
9	448	445	577	636	15900	120	581	170[h]	3.8
	(227)	(205)	(0.70)	(0.48)	(9840)	(82)		(720)	
10	459	455	583	638	81100	560	587	800[i]	6.0
	(1159)	(1154)	(0.70)	(0.07)	(8080)	(56)		(780)	
11	452	447	584	635	23000	170	586	230[j]	4.0
	(319)	(318)	(0.72)	(0.16)	(5090)	(37)		(780)	

[a] Measured in a 1×10^{-5} M solution. [b] Measured in a 1×10^{-6} M solution. [c] Fluorescent quantum yield relative to rhodamine B in ethanol (0.65). [d] In toluene solution, whereas the value in parentheses is in dichloromethane. [e] $\lambda_{ex}=800$ nm in toluene solution. [f] The maximal TPA cross-sections (σ) in toluene were estimated by using AF-50 (61 GM at 780 nm) (3.3×10^{-3} M) as a reference. The value in parentheses is absorption wavelength. 1 GM $=1\times10^{-50}$ cm^4s per photon per molecule. [g] Measured in a 1.5×10^{-3} M toluene solution. [h] Measured in a 2.0×10^{-3} M toluene solution. [i] Measured in a 1.0×10^{-3} M toluene solution. [j] Measured in a 3.3×10^{-3} M toluene solution.

As described above, the present BTD dyes can emit orange-red light. In polar dichloromethane, the emitting ability significantly changed depending on the molecular structure of the BTD dyes. In **1a**–**e** with only a benzene spacer, the φ_f value was affected by the substituents on the nitrogen atom. The highest φ_f value was observable in **1d** with 2-naphthyl groups to be 0.64 in nonpolar toluene and 0.52 in polar dichloromethane solution. Compared with **1c**–**e** with two diarylamino groups, **1a** with two dimethylamino whereas it is comparable to that (7020) of a good emitter **1c** (Tables 1 and 2).[18] Star-burst-type BTD **8** with a rigid benzene core exhibits the highest $\varepsilon\times\varphi_f$ value (27800) among all the BTD derivatives in dichloromethane. In contrast, in toluene the order of φ_f values was appropriately reflected on that of $\varepsilon\times\varphi_f$ values because of considerably high φ_f values of all the BTD derivatives. Thus, **10** shows the highest $\varepsilon\times\varphi_f$ value (81100), reflecting both high ε and φ_f values in toluene.

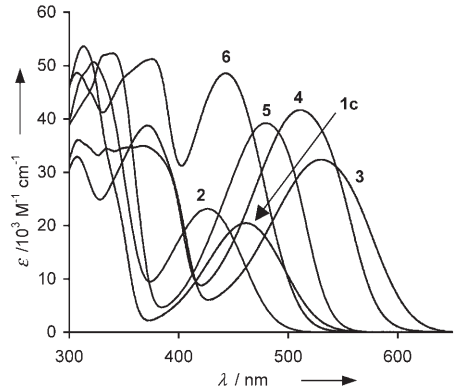

Figure 1. Single-photon absorption spectra of **1c** and **2–6** in toluene at 1×10^{-5} M.

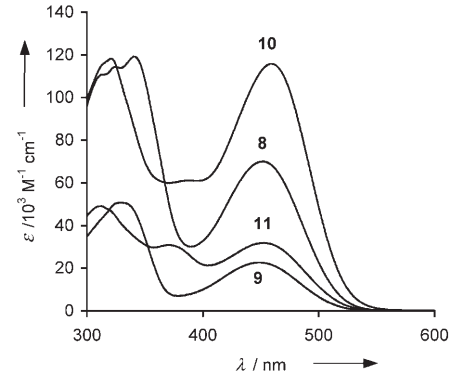

Figure 2. Single-photon absorption spectra of **8–11** in toluene at 1×10^{-5} M.

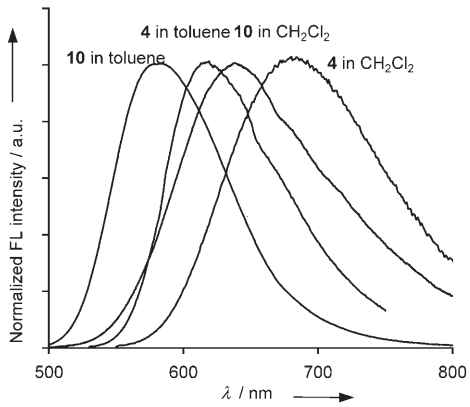

Figure 3. Single-photon excited fluorescence spectra of **4** and **10** in toluene and dichloromethane at 1×10^{-6} M.

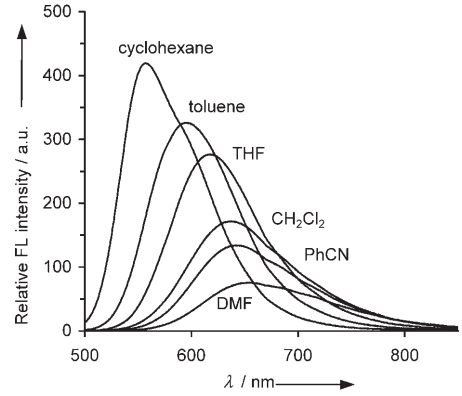

Figure 4. Single-photon excited fluorescence spectra of **1c** in cyclohexane, toluene, THF, dichloromethane, benzonitrile, and DMF at 1×10^{-6} M.

Table 3. Charge-transfer absorption and emission wavelength of **1c** in different solvents.

	Cyclo hexane	Toluene	THF	CH_2Cl_2	PhCN	DMF
λ_{max}/nm	460	461	460	459	467	460
$(10^{-2}\varepsilon)$[a]	(189)	(205)	(207)	(195)	(197)	(187)
λ_{SPEF}/nm[b]	557	592	619	639	643	657
(φ_f[c])	(0.85)	(0.62)	(0.51)	(0.36)	(0.34)	(0.22)

[a] Measured in a 1×10^{-5} M solution. [b] Measured in a 1×10^{-6} M solution. [c] Fluorescent quantum yield relative to rhodamine B in ethanol (0.65).

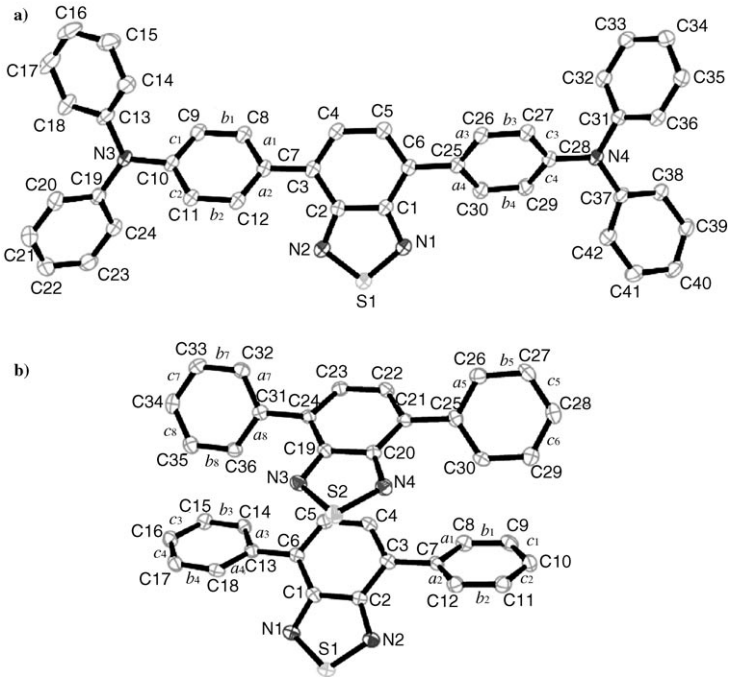

Figure 5. ORTEP drawings of a) **1c** and b) **7**.

Structural properties of BTDs: The pronounced ICT character of BTD derivatives was supported by X-ray crystallographic analysis. Single crystals of **1c** and **7**[34a] with and without the donating amino groups, respectively, were grown by slow diffusion of hexane into chloroform solutions (Figure 5). The bond-length alternation in the spacer benzene rings is a good indication for the ICT from the amino groups (donor) to the BTD ring (acceptor), which can be expressed by the quinoid character (δ_r) of the ring defined by[11]

$$\delta_r = \{(a_n - b_n) + (c_n - b_n)\}/2$$

where a_n, b_n, and c_n ($n = 1$–8) are the C–C bond lengths in the benzene ring (see Figure 5 and Table 4). As expected, the normalized δ_r value (0.0185) of **1c** is higher by one order of magnitude compared with that (0.00194) of **7**. The ICT character is reflected also in the bond length between the BTD ring and the spacer benzene ring. In **7**, the bond lengths are 1.498(4), 1.495(4), 1.500(4), and 1.497(4) Å in C3–C7, C6–C13, C21–C25, and C24–C31, respectively. In contrast, the corresponding bond lengths of C3–C7 and C6–C25 in **1c** are reduced to 1.475(3). These results indicate that the connection of the electron-donating amino group to the electron-accepting BTD ring via the π-conjugated spacer is crucial for the highly-enhanced ICT character in BTD derivatives.

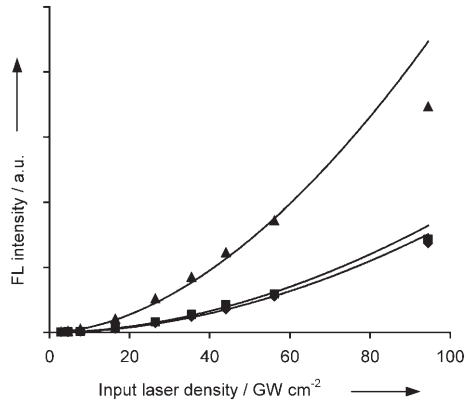

Figure 6. Dependence of the output fluorescence intensity on the input laser density in **1a** (■), **1c** (▲), and AF-50 (◆).

Two-photon absorption and emission properties: Two-photon excited fluorescence (TPEF) spectra of BTD derivatives were recorded in toluene solution at 298 K. To reduce the possibility of excited state absorption, a femtosecond Ti/sapphire laser with the pulse width of 120 fs was adopted as the excitation source in this TPEF experiment. Upon excitation at 800 nm laser pulses, all the BTDs emitted frequency-upconverted orange-red fluorescence at the wavelength region of 552–670 nm (Tables 1 and 2). For the TPEF measurement, the dependence of the output fluorescence intensity on the input laser density fits to square parabolas. Selected examples **1a** and **1c** are shown in Figure 6 together with AF-50 having D–π–A structure, which is a typical TPA material developed by Prasad's group.[12a] The result shows that the orange-red fluorescence observed in BTD derivatives was derived from two-photon excitation. When the input laser density is above a certain threshold, for example, 94 GW cm^{-2} for **1c**, the square-dependence begins to deviate, implying that some uncertain photophysical processes which cause fluorescence saturation are involved as reported previously.[13b] The TPEF bands (λ_{TPEF}) of BTD derivatives shifted to longer wavelength by 2–25 nm compared with the SPEF bands (λ_{SPEF}) (Tables 1 and 2). The red-shift is attributed to the re-absorption of the fluorescence under the concentrated solution conditions (~10^{-3} M).[18,39] As an example, a set of SPA, SPEF, and TPEF spectra of **4** was shown in Figure 7, in which the shorter wavelength region of the SPEF band partially overlaps with the tail of the linear absorption peak to effect the re-absorption. Considering this finding, one can conclude that SPEF and TPEF come from the same fluorescence excited state, although the energy level of the two-photon excited state is higher than that of the single-

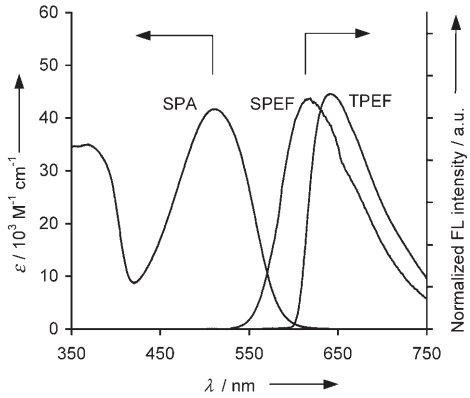

Figure 7. Single-photon absorption (SPA, at 1×10^{-5} M), single-photon excited fluorescence (SPEF, at 1×10^{-6} M), and two-photon excited fluorescence (TPEF, at 2×10^{-3} M) spectra of **4** in toluene.

Table 4. Selected bond length [Å] in **1c** and **7**.

1c					
C7–C8 (a_1)	1.399(3)	C8–C9 (b_1)	1.378(2)	C9–C10 (c_1)	1.400(3)
C7–C12 (a_2)	1.398(3)	C11–C12 (b_2)	1.388(2)	C10–C11 (c_2)	1.397(2)
C25–C26 (a_3)	1.402(3)	C26–C27 (b_3)	1.383(3)	C27–C28 (c_3)	1.399(3)
C25–C30 (a_4)	1.402(3)	C29–C30 (b_4)	1.388(3)	C28–C29 (c_4)	1.396(3)
C3–C7	1.475(3)	C6–C25	1.477(3)		
7					
C7–C8 (a_1)	1.402(3)	C8–C9 (b_1)	1.386(4)	C9–C10 (c_1)	1.390(5)
C7–C12 (a_2)	1.406(4)	C11–C12 (b_2)	1.393(4)	C10–C11 (c_2)	1.392(3)
C13–C14 (a_3)	1.403(4)	C14–C15 (b_3)	1.393(4)	C15–C16 (c_3)	1.389(3)
C13–C18 (a_4)	1.400(3)	C17–C18 (b_4)	1.396(4)	C16–C17 (c_4)	1.386(5)
C25–C26 (a_5)	1.402(4)	C26–C27 (b_5)	1.397(4)	C27–C28 (c_5)	1.390(5)
C25–C30 (a_6)	1.397(4)	C29–C30 (b_6)	1.398(4)	C28–C29 (c_6)	1.388(4)
C31–C32 (a_7)	1.397(5)	C32–C33 (b_7)	1.393(4)	C33–C34 (c_7)	1.396(4)
C31–C36 (a_8)	1.406(4)	C35–C36 (b_8)	1.397(4)	C34–C35 (c_8)	1.387(5)
C3–C7	1.498(4)	C6–C13	1.495(4)		
C21–C25	1.500(4)	C24–C31	1.497(4)		

photon excited state due to the different spectral selection rule in centro-symmetrical molecules. The λ_{TPEF} values of all the BTD derivatives are independent of the excitation wavelength from 700 to 800 nm of the tunable laser, but the TPEF intensity evidently depends on the wavelength.

TPA cross-sections (σ) of all the BTD derivatives at 700–800 nm were determined by open aperture *Z*-scan technique.[33] As a whole, plots of TPA cross-sections against the excitation wavelength exhibited two maxima around 720 and 780 nm corresponding to the π–π* and CT transitions observed in the SPA spectra (Figures 8–10), which indicate

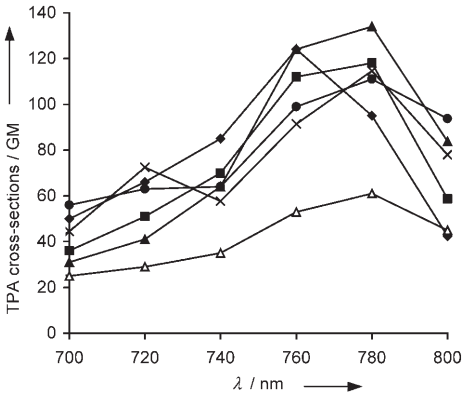

Figure 8. Two-photon absorption spectra of **1a–e** (**a**: ◆, **b**: ■, **c**: ▲, **d**: ×, **e**: ●) and AF-50 (△) in toluene.

the spectral similarity between SPA and TPA. The TPA maxima are observed at shorter wavelength positions compared to the SPA maxima, because the TPA-allowed excited state exists above the SPA excited state for this kind of centrosymmetrical molecules.

As summarized in Tables 1 and 2, all BTD derivatives exhibited large σ values around the near IR region derived from ICT compared to AF-50 used as a TPA benchmark.[12a] Figure 8 shows the plots of TPA cross-sections of **1a–e** with various substituents on the nitrogen atom. The maximal σ values of **1a–e** (110–130 GM) were about two times larger than that of AF-50 (61 GM) (Table 1). The substituents such as methyl, phenyl, 1-naphthyl, and 2-naphthyl groups on the nitrogen atom slightly affect the maximal σ values and TPA peaks.

Contrary to the effect of substituents on the nitrogen atom in **1a–e**, the expansion of π-conjugation between the BTD unit and the amino groups is crucial in increasing TPA cross-sections. The maximum σ values of **2–6** with the additional π-conjugated spacers are about 1.5–2.5 times larger than that of **1c** (Figure 9). The most significant TPA enhancement is achieved by the additional ethene spacers in **4** and **6** with σ value of 330 GM. By contrast, the introduction of the additional benzene spacer in **2** (200 GM) and the ethyne spacer in **5** (200 GM) provides moderate TPA enhancement. Interestingly, the introduction of the thiophene spacer in **3** (280 GM) moderately increases the σ value,

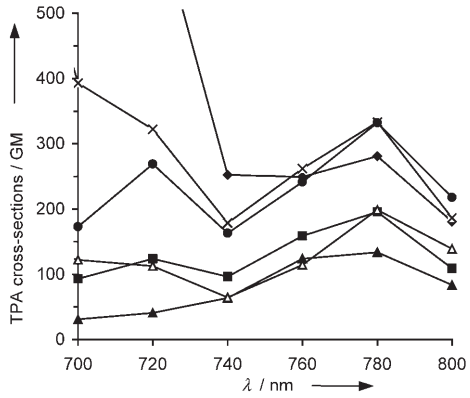

Figure 9. Two-photon absorption spectra of **1c** (▲) and **2–6** (**2**: ■, **3**: ▲, **4**: ×, **5**: △, **6**: ◆) in toluene. The σ values of **3** at 700 and 720 nm (1300 and 670 GM, respectively) are out of range of the plot area to keep clarity of other data.

which probably is correlated with the less steric hindrance between the BTD core and the thiophene ring as well as the high electron-donating ability of the thiophene ring. These observations suggest that the planarity of π-conjugated spacers affects also the TPA cross-sections. In **3** and **4**, the significant increase of σ values observed below 740 nm is interpreted as one-photon resonance enhancement on two-photon transition at a short wavelength near single-photon transition, as reported in the precedent report (Figure 9).[40] In particular, **3** provides the extremely large σ values of 1300 GM at 700 nm and 670 GM at 720 nm.

The influence of solvent polarity on the TPA characteristics of BTD derivatives was investigated by measuring TPA cross-sections of **1c** in various solvents by 800 nm excitation. The σ values of **1c** are almost the same in toluene, THF, and DMF (83, 84, and 69 GM, respectively), although the value (110 GM) in dichloromethane was slightly larger than in other solvents (Table 5). The result implies that the exci-

Table 5. Dependence of TPA cross-sections (σ) and TPEF maxima (λ_{TPEF}) of **1c** on the solvent polarity by excitation at 800 nm.

	Toluene	THF	CH_2Cl_2	DMF
σ/GM[a]	83	84	110	69
λ_{TPEF}/nm	599	617	648	673

[a] TPA cross-sections (σ) were estimated by using AF-50 (45 GM at 800 nm, in toluene) as a reference.

tation process in TPA is hardly affected by the solvent polarity. The finding can be rationalized by the less polar structure of the ground state compared with that of the excited state as found in SPA (Table 3). The TPEF spectra of **1c** display a significant red-shift from 599 to 673 nm proportional to the solvent polarity as observed in SPEF (Table 5).

Figure 10 shows the plots of TPA cross-sections of three-branched star-burst-type BTDs **8** and **10**, and their one-dimensional sub-units **9** and **11**. The maximal σ value (780 GM) of **8** with a benzene core is about 4.6 times larger than that (170 GM) of **9**. Similarly, the maximal σ value

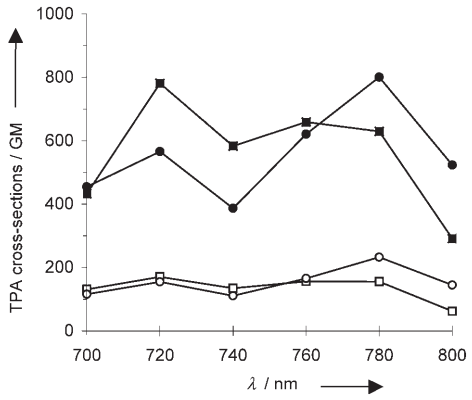

Figure 10. Two-photon absorption spectra of **8**–**11** (**8**: ■, **9**: □, **10**: ■, **11**: ◇) in toluene.

(800 GM) of **10** with a triphenylamine core is about 3.4 times larger than that (230 GM) of **11**. One can conclude that the increasing π-conjugation length as well as multidimensionality leads to cooperatively increasing the TPA cross-sections in **8** and **10**. In order to precisely discuss the TPA enhancement, the σ values were normalized to the number of π-electrons (e_π) to obtain a parameter of σ/e_π.[30] The ratio of σ/e_π values between three-branched and one-dimensional BTD derivatives are 6.5:3.8 (1.7-fold enhancement) in benzene core system **8** and **9**, and 6.0:4.0 (1.5-fold enhancement) in triphenylamine core system **10** and **11** (Table 2). The observed trend of 1.5–1.7-fold enhancement is larger than that predicted simply on the basis of the chromophore number density (i.e., 1:1) according to the increasing of branch numbers from one to three. Similar TPA enhancement in the star-burst structure was reported for triphenylamine core[25a,c,g] and triazine core systems.[27b,c] Compared with the previous examples, the present BTD derivatives provide a comparable cooperative effect in the three-branched structure, although a significant TPA enhancement of 13–23-fold was achieved in a polar pyridinium core system.[30] It can be emphasized that the TPA enhancement achieved in **8** is the first example of a benzene core, which has weaker electron-donating and accepting abilities compared with the previous triphenylamine and triazine cores, respectively.

For the development to two-photon laser scanning fluorescence imaging, the product of $\varphi_f \times \sigma$ in two-photon absorbing fluorophore is an important factor,[8a,e,19a,41] when the φ_f values in both SPA and TPA process are assumed to be the same. As summarized in Tables 1 and 2, the order of σ values was appropriately reflected on that of $\varphi_f \times \sigma$ values in toluene solution because of the relatively high φ_f values of all the BTD derivatives. Thus, star-burst **8** and **10** exhibit quite large $\varphi_f \times \sigma$ values (560 GM) compared with any other D–π–A–π–D-type derivatives, for example, **1c** (83 GM) and **4** (220 GM). In dichloromethane, the $\varphi_f \times \sigma$ value (310 GM) of **8** is still larger by one order of magnitude than those (16–77 GM) of other D–π–A–π–D-type derivatives, even under the unfavored polar conditions for fluorescence emitting. In contrast, **10** shows low $\varphi_f \times \sigma$ value of 56 GM because of its low φ_f value.

Conclusion

In conclusion, we have demonstrated that a series of D–π–A–π–D-type and star-burst-type benzothiadiazole-based dyes possessing terminal *N*,*N*-disubstituted amino groups provide high fluorescence quantum yields among the orange-red color region as well as large two-photon absorption cross-sections in the near IR region. The two-photon absorption activity is attributed to the electron-accepting nature of the benzothiadiazole unit, which causes significant intramolecular charge-transfer even in the ground state by the combination with the electron-donating amino groups connected with the π-conjugated spacers. Further, the extended π-conjugate system including the donor and acceptor moieties lowers the excited state to emit the attractive red-orange fluorescence. In the D–π–A–π–D system, the length and planarity of the π-conjugated spacers between the benzothiadiazole unit and the amino groups play an important role in increasing the two-photon absorption activity. In addition, the combination of dimensionality and extended π-system leads to significant increase of the two-photon absorption cross-sections in star-burst structure. The present benzothiadiazole-based two-photon absorbing dyes with red-orange fluorescence emitting ability are attractive candidates as a new material toward two-photon laser scanning microscopy. However, we need more efforts to create a useful optical emission window in near IR region (650–900 nm) for fluorescence bioimaging.[42,43] We believe that the present study provides valuable information for the synthesis of new two-photon absorbing materials.

Experimental Section

General methods: All melting points are uncorrected. IR spectra were recorded on a JASCO FT/IR-470 plus Fourier transform infrared spectrometer and measured as KBr pellets. ^{1}H NMR spectra were determined in $CDCl_3$ or [D_6]DMSO with a JEOL EX-270, and GSX-270 spectrometer. Residual solvent protons were used as internal standard and chemical shifts (δ) are given relative to tetramethylsilane (TMS). The coupling constants (J) are given in Hertz. Elemental analysis was performed at the Elemental Analytical Center, Kyushu University. EI-MS spectra were recorded with a JEOL JMS-70 mass spectrometer at 70 eV using a direct inlet system. FAB-MS spectra were recorded with a JEOL JMS-70 mass spectrometer with *m*-nitrobenzyl alcohol as a matrix. Matrix assisted laser desorption ionization time-of-flight (MALDI-TOF) mass spectrometry was performed on a PerSeptive Biosystems Voyager-DE spectrometer by using delayed extraction mode and with an acceleration voltage of 20 keV. Samples were prepared from a solution of dichloromethane by using dithranol as the matrix. UV/Vis spectra were measured on a JASCO V-570 spectrophotometer in a 1 cm width quartz cell. Fluorescence spectra were measured on a HITACHI F-4500 fluorescence spectrophotometer in a 1 cm width quartz cell. Gel-permeation chromatography (GPC) was performed with a Japan Analytical Industry Co., Ltd. LC-908 using JAIGEL-1H column (20×600 mm) and JAIGEL-2H column (20×600 mm) eluting with chloroform (3.5 mL min^{-1}). Analytical TLC was carried out on silica gel coated on aluminum foil (Merck 60

F_{254}). Column chromatography was carried out on silica gel (Wako C-300 or KANTO 60N). THF was distilled from sodium and benzophenone under an argon atmosphere just before use. DMF was distilled from calcium hydride under reduced pressure just before use. Benzene was dried with 4 Å molecular sieve over night before use. 4-Dimethylaminophenylboronic acid (**13a**) and 4-diphenylaminobenzaldehyde (**22**) are commercially available. 4,7-Dibromo-2,1,3-benzothiadiazole (**12**),[44] *N*-(4-bromophenyl)-1-naphthylphenylamine,[45] 4-(*N*,*N*-diphenylamino)phenylboronic acid (**13b**),[46] 4-[*N*-(2-naphthyl)-*N*-phenyl]phenylboronic acid (**13d**),[47] 4-(*N*,*N*-diphenylamino)biphenyl-4′-boronic acid (**13e**),[48] 4,7-bis(5-bromo-2-thienyl)-2,1,3-benzothiadiazole (**14**),[35] 1-(*N*,*N*-diphenylamino)-4-vinylbenzene (**15**),[49] 4-diphenylaminoiodobenzene (**18**),[45] 4,7-bis[(4-hydroxymethyl)phenyl]-2,1,3-benzothiadiazole (**19**),[37] 4-[4-(*N*,*N*-diphenylamino)-phenyl]-7-(4-formylphenyl)-2,1,3-benzothiadiazole (**23**),[38] 1,3,5-tris(dimethoxyphosphorylmethyl)benzene (**27**),[50] and tris(4-formylphenyl)amine (**29**)[51] were prepared according to methods described previously. Benzyltriphenylphosphonium bromide (**28**) was prepared from benzyl bromide and triphenylphosphine according to common method. Preparation of **1c** and **3** were reported by another group by using Stille coupling reactions.[35]

4-Bromo-7-[4-(*N*,*N*-dimethylamino)phenyl]-2,1,3-benzothiadiazole: A solution of **13a** (400 mg, 3.40 mmol) in ethanol (5 mL) and aqueous 2 M Na_2CO_3 (25 mL) were added at 60 °C under an argon atmosphere to a mixture of **12** (1.00 g, 3.40 mmol) and tetrakis(triphenylphosphine)palladium(0) (118 mg, 0.10 mmol) in benzene (50 mL). After the mixture was heated at 85 °C for 12 h, the reaction mixture was poured into water (120 mL) and extracted with toluene (40 mL × 3). The combined organic layers were dried over anhydrous magnesium sulfate and evaporated in vacuo to dryness. The residue was purified by silica gel column chromatography (Wako C-300) eluting with chloroform/hexane 2:5 and recrystallization from chloroform/hexane to give 4-bromo-7-[4-(*N*,*N*-dimethylamino)phenyl]-2,1,3-benzothiadiazole (772 mg, 2.31 mmol, 68 %) as orange prisms. M.p. 179–180 °C; ^{1}H NMR (270 MHz, $CDCl_3$, 25 °C, TMS): δ = 3.05 (s, 6H; CH_3), 6.86 (d, J = 8.9 Hz, 2H; ArH), 7.51 (d, J = 7.6 Hz, 1H; ArH), 7.83–7.88 ppm (m, 3H; ArH); IR (KBr): $\tilde{\nu}$ = 1609, 1513, 1479, 1362, 1200, 884, 810 cm^{-1}; EI-MS (70 eV): m/z: 333, 335 [M^+]; elemental analysis calcd (%) for $C_{14}H_{12}N_3BrS$ (334.2): C 50.31, H 3.62, N 12.57; found: C 50.31, H 3.60, N 12.55.

4,7-Bis[4-(*N*,*N*-dimethylamino)phenyl]-2,1,3-benzothiadiazole (1a): An solution of **13a** (138 mg, 0.83 mmol) in ethanol (2 mL) and aqueous 2 M Na_2CO_3 (25 mL) were added at 60 °C under an argon atmosphere to a mixture of 4-bromo-7-[4-(*N*,*N*-dimethylamino)phenyl]-2,1,3-benzothiadiazole (200 mg, 0.60 mmol) and tetrakis(triphenylphosphine)palladium(0) (21 mg, 0.018 mmol) in benzene (20 mL). After the mixture was heated at 85 °C for 12 h, the reaction mixture was poured into water (100 mL). The precipitates were collected by filtration and washed well with water and benzene to give **1a** (130 mg, 0.35 mmol, 58 %) as red needles. An analytical sample was obtained by gel-permeation chromatography eluting with chloroform. M.p. 217–218 °C; ^{1}H NMR (270 MHz, $CDCl_3$, 25 °C, TMS): δ = 3.04 (s, 12H; CH_3), 6.89 (d, J = 8.5 Hz, 4H; ArH), 7.68 (s, 4H; ArH), 7.91 ppm (d, J = 8.5 Hz, 2H; ArH); IR (KBr): $\tilde{\nu}$ = 1611, 1528, 1478, 1444, 1364, 1229, 1202, 1113, 811 cm^{-1}; FAB-MS (NBA): m/z: 374 [M^+]; elemental analysis calcd (%) for $C_{22}H_{22}N_4S$ (374.5): C 70.56, H 5.92, N 14.96; found: C 70.31, H 5.68, N 15.06.

4-[4-(*N*,*N*-Dimethylamino)phenyl]-7-[4-(*N*,*N*-diphenylamino)phenyl]-2,1,3-benzothiadiazole (1b): A solution of **13b** (155 mg, 0.53 mmol) in ethanol (2 mL) and aqueous 2 M Na_2CO_3 (20 mL) were added at 60 °C under an argon atmosphere to a mixture of 4-bromo-7-[4-(*N*,*N*-dimethylamino)phenyl]-2,1,3-benzothiadiazole (150 mg, 0.44 mmol) and tetrakis(triphenylphosphine)palladium(0) (15 mg, 0.013 mmol) in benzene (30 mL). After the mixture was heated at 85 °C for 12 h, the reaction mixture was poured into water (150 mL) and extracted with toluene (30 mL × 3). The combined organic layers were dried over anhydrous magnesium sulfate and evaporated in vacuo to dryness. The residue was purified by silica gel column chromatography (KANTO 60N) eluting with toluene to give **1b** (162 mg, 0.32 mmol, 73 %) as an orange powder. An analytical sample was obtained by gel-permeation chromatography eluting with chloroform. M.p. 245–247 °C; ^{1}H NMR (270 MHz, $CDCl_3$, 25 °C, TMS): δ = 3.05 (s, 6H; CH_3), 6.89 (d, J = 8.6 Hz, 2H; ArH), 7.05 (t, J = 7.3 Hz, 2H; ArH), 7.16–7.32 (m, 10H; ArH), 7.70 (d, J = 7.6 Hz, 1H; ArH), 7.73 (d, J = 7.6 Hz, 1H; ArH), 7.88 (d, J = 8.6 Hz, 2H; ArH), 7.93 ppm (d, J = 8.6 Hz, 2H; ArH); IR (KBr): $\tilde{\nu}$ = 1610, 1590, 1489, 1349, 1282, 1197, 887, 813 cm^{-1}; EI-MS (70 eV): m/z: 498 [M^+]; elemental analysis calcd (%) for $C_{32}H_{26}N_4S$ (498.6): C 77.08, H 5.26, N 11.24; found: C 76.81, H 5.28, N 11.16.

4,7-Bis[4-(*N*,*N*-diphenylamino)phenyl]-2,1,3-benzothiadiazole (1c):[35] A solution of **13b** (112 mg, 0.18 mmol) in ethanol (3 mL) and aqueous 2 M Na_2CO_3 (10 mL) were added at 60 °C under an argon atmosphere to a mixture of **12** (46 mg, 0.16 mmol) and tetrakis(triphenylphosphine)palladium(0) (5.5 mg, 0.0048 mmol) in benzene (20 mL). After the mixture was heated at 85 °C for 12 h, the reaction mixture was poured into water (50 mL) and extracted with toluene (30 mL × 3). The combined organic layers were dried over anhydrous magnesium sulfate and evaporated in vacuo to dryness. The residue was separated by silica gel column chromatography (KANTO 60N) eluting with chloroform/hexane 1:2 to give an orange powder (50 mg), which was the mixture of **1c** and 4-bromo-7-[4-(*N*,*N*-diphenylamino)phenyl]-2,1,3-benzothiadiazole. To a mixture of this orange powder (50 mg) and tetrakis(triphenylphosphine)palladium(0) (3.8 mg, 0.0033 mmol) in benzene (15 mL) were added a solution of **13b** (124 mg, 0.21 mmol) in ethanol (1 mL) and aqueous 2 M Na_2CO_3 (7 mL) at 60 °C under an argon atmosphere. After the mixture was heated at 85 °C for 12 h, the reaction mixture was poured into water (50 mL) and extracted with toluene (20 mL × 3). The combined organic layers were dried over anhydrous magnesium sulfate and evaporated in vacuo to dryness. The residue was purified by silica gel column chromatography (KANTO 60N) eluting with chloroform/hexane 1:2 to give **1c** (52 mg, 0.084 mmol, 53 %) as a red powder. An analytical sample was obtained by gel-permeation chromatography eluting with chloroform. M.p. 236–238 °C; ^{1}H NMR (270 MHz, $CDCl_3$, 25 °C, TMS): δ = 7.06 (t, J = 8.5 Hz, 4H; ArH), 7.17–7.32 (m, 20H; ArH), 7.74 (s, 2H; ArH), 7.88 ppm (d, J = 8.5 Hz, 4H; ArH); IR (KBr): $\tilde{\nu}$ = 1590, 1513, 1484, 1328, 1278, 825, 754 cm^{-1}; FAB-MS (NBA): m/z: 622 [M^+]; elemental analysis calcd (%) for $C_{42}H_{30}N_4S$ (622.8): C 81.00, H 4.86, N 9.00; found: C 80.79, H 4.87, N 9.02.

4,7-Bis{4-[*N*-(1-naphthyl)-*N*-phenylamino]phenyl}-2,1,3-benzothiadiazole (1d): According to a method similar to the preparation of **1c**, **1d** was obtained in 73 % yield from **12** and **13c**. The crude product was purified by silica gel column chromatography (KANTO 60N) eluting with chloroform/hexane 3:2. An analytical sample was obtained by gel-permeation chromatography eluting with chloroform as a red powder. ^{1}H NMR (270 MHz, $CDCl_3$, 25 °C, TMS): δ = 7.10 (t, J = 7.3 Hz, 2H; ArH), 7.22–7.45 (m, 18H; ArH), 7.54–7.66 (m, 4H; ArH), 7.75–7.80 (m, 4H; ArH), 7.78 (s, 2H; ArH), 7.92 ppm (d, J = 8.6 Hz, 4H; ArH); IR (KBr): $\tilde{\nu}$ = 1592, 1508, 1480, 1279, 811, 747 cm^{-1}; FAB-MS (NBA): m/z: 722 [M^+]; elemental analysis calcd (%) for $C_{50}H_{34}N_4S \cdot 0.1\,CHCl_3$ (734.8): C 81.89, H 4.68, N 7.62; found: C 82.18, H 4.85, N 7.35.

4,7-Bis{4-[*N*-(2-naphthyl)-*N*-phenylamino]phenyl}-2,1,3-benzothiadiazole (1e): According to a method similar to the preparation of **1c**, **1e** was obtained in 53 % yield from **12** and **13d**. The crude product was purified by silica gel column chromatography (KANTO 60N) eluting with chloroform/hexane 3:2. An analytical sample was obtained by gel-permeation chromatography eluting with chloroform as a red powder. ^{1}H NMR (270 MHz, $CDCl_3$, 25 °C, TMS): δ = 7.10 (t, J = 7.3 Hz, 2H; ArH), 7.22–7.45 (m, 18H; ArH), 7.54–7.66 (m, 4H; ArH), 7.75–7.80 (m, 4H; ArH), 7.78 (s, 2H; ArH), 7.92 ppm (d, J = 8.6 Hz, 4H; ArH); IR (KBr): $\tilde{\nu}$ = 1592, 1508, 1480, 1279, 811, 747 cm^{-1}; FAB-MS (NBA): m/z: 722 [M^+]; elemental analysis calcd (%) for $C_{50}H_{34}N_4S \cdot 0.1\,CHCl_3$ (734.8): C 81.89, H 4.68, N 7.62; found: C 81.86, H 4.53, N 7.63.

4,7-Bis(4′-*N*,*N*-diphenylaminobiphenyl-4-yl)-2,1,3-benzothiadiazole (2): According to a method similar to the preparation of **1c**, **2** was obtained in 18 % yield from **12** and **13e**. The crude product was purified by silica gel column chromatography (KANTO 60N) eluting with chloroform/hexane 1:1. An analytical sample was obtained by gel-permeation chromatography eluting with chloroform as an orange powder. M.p. 220–222 °C; ^{1}H NMR (270 MHz, $CDCl_3$, 25 °C, TMS): δ = 7.05 (t, J = 7.1 Hz, 4H; ArH), 7.14–7.33 (m, 20H; ArH), 7.57 (d, J = 8.9 Hz, 4H; ArH), 7.76

(d, $J=8.4$ Hz, 4H; ArH), 7.86 (s, 2H; ArH), 8.06 ppm (d, $J=8.4$ Hz, 4H; ArH); IR (KBr): $\tilde{\nu}=3030$, 1590, 1480, 1329, 1280, 816, 754 cm^{-1}; FAB-MS (NBA): m/z: 774 [M^+]; elemental analysis calcd (%) for $C_{54}H_{38}N_4S$ (774.9): C 83.69, H 4.94, N 7.23; found: C 83.70, H 4.93, N 7.26.

4,7-Bis{5-[4-(*N*,*N*-diphenylamino)phenyl]-2-thienyl}-2,1,3-benzothiadiazole (3):[35] A solution of **13b** in ethanol (1 mL) and aqueous 2 M Na_2CO_3 (2 mL) were added at 70 °C under an argon atmosphere to a mixture of **14** (115 mg, 0.25 mmol) and tetrakis(triphenylphosphine)palladium(0) (25 mg, 0.25 mmol) in benzene (4 mL). After the mixture was heated at 85 °C for 24 h, the reaction mixture was concentrated in vacuo to remove benzene. The residue was extracted with chloroform (50 mL × 3), dried over anhydrous magnesium sulfate, and evaporated in vacuo to dryness. The residue was recrystallized from chloroform/hexane and purified by gel-permeation chromatography eluting with chloroform to give **3** (65 mg, 0.08 mmol, 33 %) as a red powder. M.p. 262–264 °C; ^{1}H NMR (270 MHz, $CDCl_3$, 25 °C, TMS): $\delta=7.00$–7.18 (m, 20H; ArH), 7.27–7.37 (m, 6H; ArH), 7.55 (d, $J=8.6$ Hz, 4H; ArH), 7.86 (s, 2H; ArH), 8.11 ppm (d, $J=4.0$ Hz, 2H; ArH); IR (KBr): $\tilde{\nu}=1590$, 1483, 1448, 1325, 1279, 835, 795, 755, 695, 515 cm^{-1}; FAB-MS (NBA): m/z: 786 [M^+]; elemental analysis calcd (%) for $C_{50}H_{34}N_4S_3\cdot0.15\,CHCl_3$ (804.9): C 74.83, H 4.28, N 6.96; found: C 74.82, H 4.26, N 7.05.

4,7-Bis{2-[4-(*N*,*N*-diphenylamino)phenyl]-(*E*)-ethenyl}-2,1,3-benzothiadiazole (4): A solution of tris(*o*-tolyl)phosphine (3 mg, 0.01 mmol) and palladium acetate (2 mg, 0.005 mmol) in dry DMF (5 mL) was added dropwise at 80 °C under an argon atmosphere to a solution of **12** (74 mg, 0.25 mmol), **15** (150 mg, 0.55 mmol) in triethylamine (1 mL) and dry DMF (15 mL). After the mixture was heated at 110 °C for 12 h, the reaction mixture was poured into water (50 mL), and extracted with chloroform (40 mL × 3). The combined organic layers were neutralized with 1.2 N aqueous HCl (20 mL), washed with brine (30 mL × 3), dried over anhydrous magnesium sulfate, and evaporated in vacuo to dryness. The residue was purified by silica gel column chromatography (KANTO 60N) eluting with chloroform/hexane 4:3 to give **4** (28 mg, 0.04 mmol, 17 %) as a red glass. An analytical sample was obtained by gel-permeation chromatography eluting with chloroform. M.p. 196–198 °C; ^{1}H NMR (270 MHz, $CDCl_3$, 25 °C, TMS): $\delta=7.02$–7.16 (m, 16H; ArH), 7.27 (d, $J=7.3$ Hz, 4H; ArH), 7.29 (d, $J=8.6$ Hz, 4H; ArH), 7.52 (d, $J=8.6$ Hz, 4H; ArH), 7.54 (d, $J=16.2$ Hz, 2H; olefinic H), 7.65 (s, 2H; ArH), 7.92 ppm (d, $J=16.2$ Hz, 2H; olefinic H); IR (KBr): $\tilde{\nu}=1589$, 1507, 1591, 1326, 1281, 1175, 963 cm^{-1}; FAB-MS (NBA): m/z: 674 [M^+]; elemental analysis calcd (%) for $C_{46}H_{34}N_4S\cdot0.03\,CHCl_3$ (678.4): C 81.49, H 5.06, N 8.26; found: C 81.41, H 5.10, N 8.21.

4,7-Bis{2-[4-(*N*,*N*-diphenylamino)phenyl]ethynyl}-2,1,3-benzothiadiazole (5): A mixture of **16** (180 mg, 0.54 mmol) in 1 N potassium hydroxide methanol solution (15 mL) was stirred at room temperature for 1 h. The reaction mixture was poured into water (40 mL) and extracted with chloroform (25 mL × 3). The combined organic layers were evaporated in vacuo to dryness after dried over anhydrous magnesium sulfate to give **17** (91 mg, 0.49 mmol) as a brown powder. To a solution of **17** (91 mg, 0.49 mmol), **18** (400 mg, 1.08 mmol), and triethylamine (2 mL) in dry THF (5 mL) was added diphenylphosphinoferocene palladium dichloride (7 mg, 0.01 mmol) and copper iodide(I) (7 mg, 0.04 mmol) under an argon atmosphere. After the mixture was stirred at room temperature for 1.5 h, the reaction mixture was poured into water (50 mL) and extracted with dichloromethane (30 mL × 3). The combined organic layers were neutralized with 1.2 N HCl (20 mL), washed with brine (20 mL × 3), dried over anhydrous magnesium sulfate, and evaporated in vacuo to dryness. The residue was purified by silica gel column chromatography (KANTO 60N) eluting with dichloromethane/hexane 3:2 to give **5** (39 mg, 0.058 mmol, 11 %) as a red powder. M.p. 249–251 °C; ^{1}H NMR (270 MHz, $CDCl_3$, 25 °C, TMS): $\delta=7.03$ (d, $J=8.9$ Hz, 4H; ArH), 7.12 (t, $J=8.6$ Hz, 12H; ArH), 7.26–7.32 (m, 8H; ArH), 7.50 (d, $J=8.9$ Hz, 4H; ArH), 7.73 ppm (s, 2H; ArH); IR (KBr): $\tilde{\nu}=2198$ (C≡C), 1589, 1557, 1510, 1490, 1317, 1287, 1172, 824, 753 cm^{-1}; FAB-MS (NBA): m/z: 670 [M^+]; elemental analysis calcd (%) for $C_{46}H_{30}N_4S\cdot0.1\,CHCl_3$ (682.8): C 81.09, H 4.44, N 8.20; found: C 81.05, H 4.48, N 8.07.

4,7-Bis{4-{2-[4-(*N*,*N*-diphenylamino)phenyl]-(*E*)-ethenyl}phenyl}-2,1,3-benzothiadiazole (6): Potassium *tert*-butoxide (62 mg, 0.56 mmol) was added at room temperature under an argon atmosphere to a solution of **21** (100 mg, 0.19 mmol) and **22** (133 mg, 0.49 mmol) in dry THF (20 mL). After the mixture was stirred at room temperature for 12 h, the reaction mixture was poured into water (60 mL) and extracted with dichloromethane (30 mL × 3). The combined organic layers were dried over anhydrous magnesium sulfate and evaporated in vacuo to dryness. The residue was purified by silica gel column chromatography (KANTO 60N) eluting with chloroform/hexane 8:1 and recrystallized from chloroform/hexane to give **6** (95 mg, 0.12 mmol, 61 %) as an orange powder. M.p. 246–247 °C; ^{1}H NMR (270 MHz, $CDCl_3$, 25 °C, TMS): $\delta=7.01$–7.15 (m, 24H; ArH), 7.24 (d, $J=15.8$ Hz, 2H; olefinic H), 7.26 (d, $J=8.9$ Hz, 4H; ArH), 7.28 (d, $J=15.8$ Hz, 2H; olefinic H), 7.44 (d, $J=8.9$ Hz, 4H; ArH), 7.67 (d, $J=8.4$ Hz, 4H; ArH), 7.82 ppm (s, 2H; ArH); IR (KBr): $\tilde{\nu}=1588$, 1490, 1327, 1279, 1175, 964, 889, 829 cm^{-1}; FAB-MS (NBA): m/z: 827 [M+H$^+$]; elemental analysis calcd (%) for $C_{58}H_{42}N_4S\cdot0.07\,CHCl_3$ (835.4): C 83.48, H 5.08, N 6.71; found: C 83.40, H 5.12, N 6.75.

1,3,5-Tris{2-{4-[7-[4-(*N*,*N*-diphenylamino)phenyl]benzothiadiazolyl}phenyl}-(*E*)-ethenyl}benzene (8): Compound **23** (200 mg, 0.41 mmol) was added at room temperature under an argon atmosphere to a solution of **27** (61 mg, 0.14 mmol) and potassium *tert*-butoxide (71 mg, 0.63 mmol) in dry THF (30 mL). After the mixture was heated at 40 °C for 12 h, the reaction mixture was poured into aqueous 1.2 N HCl (100 mL) and extracted with chloroform (40 mL × 3). The combined organic layers were dried over anhydrous magnesium sulfate and evaporated in vacuo to dryness. The residue was purified by silica gel column chromatography (KANTO 60N) eluting with chloroform and recrystallized from chloroform/hexane to give **8** (130 mg, 0.088 mmol, 63 %) as a red powder. M.p. 176–178 °C; ^{1}H NMR (270 MHz, $CDCl_3$, 25 °C, TMS): $\delta=7.08$ (t, $J=7.3$ Hz, 6H; ArH), 7.19–7.34 (m, 30H; ArH), 7.68 (s, 3H; ArH), 7.77 (d, $J=8.6$ Hz, 6H; ArH), 7.79 (d, $J=7.3$ Hz, 3H; ArH), 7.80 (d, $J=15.8$ Hz, 3H; olefinic H), 7.83 (d, $J=15.8$ Hz, 3H; olefinic H), 7.85 (d, $J=7.3$ Hz, 3H; ArH), 7.90 (d, $J=8.6$ Hz, 6H; ArH), 8.06 ppm (d, $J=8.3$ Hz, 6H; ArH); IR (KBr): $\tilde{\nu}=1590$, 1481, 1280, 888, 830, 753 cm^{-1}; FAB-MS (NBA): m/z: 1517 [M^+]; elemental analysis calcd (%) for $C_{102}H_{69}N_9S_3$ (1516.8): C 80.76, H 4.58, N 8.31; found: C 80.46, H 4.65, N 8.20.

4-[4-(*N*,*N*-Diphenylamino)phenyl]-7-{[(2-phenyl)-(*E*)-ethenyl]phenyl}-2,1,3-benzothiadiazole (9): Potassium *tert*-butoxide (52 mg, 0.46 mmol) was added at room temperature under an argon atmosphere to a solution of **23** (110 mg, 0.23 mmol) and **28** (128 mg, 0.30 mmol) in dry THF (20 mL). After the mixture was stirred at room temperature for 1 h, the reaction mixture was poured into water (60 mL) and extracted with dichloromethane (30 mL × 3). The combined organic layers were dried over anhydrous magnesium sulfate and evaporated in vacuo to dryness. The residue was purified by silica gel column chromatography (KANTO 60N) eluting with chloroform/hexane 1:1 and recrystallized from chloroform/hexane to give **9** (53 mg, 0.095 mmol, 41 %) as an orange powder. M.p. 247–248 °C; ^{1}H NMR (270 MHz, $CDCl_3$, 25 °C, TMS): $\delta=7.07$ (t, $J=7.3$ Hz, 2H; ArH), 7.18–7.33 (m, 13H; ArH, olefinic H), 7.39 (t, $J=7.3$ Hz, 2H; ArH), 7.57 (d, $J=7.3$ Hz, 2H; ArH), 7.70 (d, $J=8.3$ Hz, 2H; ArH), 7.77 (d, $J=7.3$ Hz, 1H; ArH), 7.82 (d, $J=7.3$ Hz, 1H; ArH), 7.90 (d, $J=8.6$ Hz, 2H; ArH), 8.01 ppm (d, $J=8.3$ Hz, 2H; ArH); IR (KBr): $\tilde{\nu}=1590$, 1489, 1285, 817, 752, 696 cm^{-1}; FAB-MS (NBA): m/z: 557 [M^+]; elemental analysis calcd (%) for $C_{38}H_{27}N_3S$ (557.7): C 81.84, H 4.88, N 7.53; found: C 81.71, H 4.90, N 7.53.

Tris{4-{2-{4-[7-(4-*N*,*N*-diphenylamino)phenyl]benzothiadiazolyl}phenyl}-(*E*)-ethenyl}phenyl}amine (10): Potassium *tert*-butoxide (38 mg, 0.34 mmol) was added at room temperature under an argon atmosphere to a solution of **26** (110 mg, 0.19 mmol) and **29** (19 mg, 0.058 mmol) in dry THF (20 mL). After the mixture was stirred at room temperature for 8 h, the reaction mixture was poured into aqueous 1.2 N HCl (50 mL) and extracted with chloroform (30 mL × 3). The combined organic layers were dried over anhydrous magnesium sulfate and evaporated in vacuo to dryness. The residue was purified by silica gel column chromatography (KANTO 60N) eluting with chloroform/hexane 5:2 and recrystallized from chloroform/hexane to give **10** (58 mg, 0.034 mmol, 59 %) as a red powder. M.p. 186–188 °C; ^{1}H NMR (270 MHz, $CDCl_3$, 25 °C, TMS): $\delta=$ 7.08 (t, $J=7.3$ Hz, 6H; ArH), 7.18–7.34 (m, 42H; olefinic H, ArH), 7.50 (d, $J=8.6$ Hz, 6H; ArH), 7.69 (d, $J=8.6$ Hz, 6H; ArH), 7.77 (d, $J=$

7.4 Hz, 3H; ArH), 7.82 (d, $J=7.4$ Hz, 3H; ArH), 7.89 (d, $J=8.9$ Hz, 6H; ArH), 8.01 ppm (d, $J=8.6$ Hz, 6H; ArH); IR (KBr): $\tilde{\nu}=2924$, 1590, 1480, 1278, 1073, 888, 824, 753, 697 cm^{-1}; MALDI-TOF-MS (dithranol): m/z: calcd for $C_{114}H_{79}N_{10}S_3$: 1683.56; found: 1683.81 $[M+H^+]$; elemental analysis calcd (%) for $C_{114}H_{78}N_{10}S_3$ (1684.1): C 81.30, H 4.67, N 8.32; found: C 80.98, H 4.79, N 8.15.

4-[4-(*N*,*N*-Diphenylamino)phenyl]-7-{4-[2-[4-(*N*,*N*-diphenylamino)phenyl]-(*E*)-ethenyl}phenyl}-2,1,3-benzothiadiazole (11): Potassium *tert*-butoxide (39 mg, 0.35 mmol) was added at room temperature under an argon atmosphere to a solution of **22** (61 mg, 0.22 mmol) and **26** (100 mg, 0.17 mmol) in dry THF (15 mL). After the mixture was stirred at room temperature for 8 h, the reaction mixture was poured into aqueous 1.2 N HCl (50 mL) and extracted with chloroform (30 mL × 3). The combined organic layers were dried over anhydrous magnesium sulfate and evaporated in vacuo to dryness. The residue was purified by silica gel column chromatography (KANTO 60N) eluting with chloroform/hexane 3:1 and recrystallized from chloroform/hexane to give **11** (81 mg, 0.11 mmol, 65%) as a red powder. M.p. 190–191 °C; ^{1}H NMR (270 MHz, $CDCl_3$, 25 °C, TMS): $\delta=7.01$–7.33 (m, 26H; olefinic H, ArH), 7.44 (d, $J=8.7$ Hz, 2H; ArH), 7.67 (d, $J=8.4$ Hz, 2H; ArH), 7.77 (d, $J=7.4$ Hz, 1H; ArH), 7.81 (d, $J=7.4$ Hz, 1H; ArH), 7.89 (d, $J=8.9$ Hz, 2H; ArH), 7.99 ppm (d, $J=8.4$ Hz, 2H; ArH); IR (KBr): $\tilde{\nu}=1590$, 1491, 1327, 1280, 1024, 825, 752 cm^{-1}; FAB-MS (NBA): m/z: 725 $[M+H^+]$; elemental analysis calcd (%) for $C_{50}H_{36}N_4S$ (724.9): C 82.84, H 5.01, N 7.73; found: C 82.84, H 4.89, N 7.70.

4-[*N*-(1-Naphthyl)-*N*-phenyl]phenylboronic acid (13c): A 2.6 M butyllithium/hexane solution (6.03 mL, 16.1 mmol) was added dropwise at −78 °C under an argon atmosphere to a solution of *N*-(4-bromophenyl)-1-naphthylphenylamine (5.48 g, 14.6 mmol) in dry THF (35 mL). After the mixture was stirred at −78 °C for 1 h, dry THF solution (5 mL) of trimethylborate (2.28 g, 21.9 mmol) was added dropwise to the mixture. The reaction mixture was stirred at −60 °C for 1 h and at room temperature for 3 h. After the mixture was quenched by addition of aqueous 3 N HCl (40 mL), it was extracted with diethyl ether (40 mL × 3). The combined organic layers were washed with brine (40 mL × 2), dried over anhydrous magnesium sulfate, and evaporated in vacuo to dryness. After the residue was suspended in hexane, it was collected by filtration and washed with hexane to give **13c** (1.75 g, 5.16 mmol, 35%) as a white powder. Without further purification, it was used in the next preparation. ^{1}H NMR (270 MHz, [D$_6$]DMSO, 25 °C, TMS): $\delta=6.96$ (d, $J=8.6$ Hz, 2H; ArH), 7.04–7.12 (m, 3H; ArH), 7.22 (dd, $J=2.3$, 8.9 Hz, 1H; ArH), 7.31–7.47 (m, 5H; ArH), 7.71 (d, $J=8.6$ Hz, 2H; ArH), 7.83–7.88 ppm (m, 3H; ArH); IR (KBr): $\tilde{\nu}=1628$, 1590, 1507, 1490, 1467, 1416, 1350 (BO), 1277, 1180, 812, 746 cm^{-1}.

4,7-Bis(trimethylsilylethynyl)-2,1,3-benzothiadiazole (16): Tetrakis(triphenylphosphine)palladium(0) (35 mg, 0.03 mmol) and copper iodide(I) (11 mg, 0.06 mmol) were added in pressure tube under an argon atmosphere to a mixture of **12** (441 mg, 15 mmol) and trimethylsilyl acetylene (0.6 mL, 4.5 mmol) in triethylamine (25 mL). After the mixture was heated at 75 °C for 5 h, the reaction mixture was poured into cold water (100 mL) and extracted with dichloromethane (30 mL × 3). The combined organic layers were washed with water (50 mL × 2) and aqueous 1.2 N HCl (30 mL), dried over anhydrous magnesium sulfate, and evaporated in vacuo to dryness. The residue was purified by silica gel column chromatography (WAKO C-300) eluting with diethyl ether/hexane 1:1 to give **16** (460 mg, 14 mmol, 98%) as a pale yellow powder. An analytical sample was obtained by recrystallization from cold methanol to give **16** as a pale yellow plate. M.p. 117–118 °C; ^{1}H NMR (270 MHz, $CDCl_3$, 25 °C, TMS): $\delta=0.33$ (s, 18H; CH_3), 7.70 ppm (s, 2H; ArH); IR (KBr): $\tilde{\nu}=2960$, 2898, 2150 (C≡C), 1538, 1490, 1412, 1357, 1338, 1248, 1167, 1062, 1027 cm^{-1}; EI-MS (70 eV): m/z: 328 $[M^+]$; elemental analysis calcd (%) for $C_{16}H_{20}N_2SSi_2$ (328.5): C 58.49, H 6.14, N 8.53; found: C 58.55, H 6.18, N 8.43.

4,7-Bis[(4-bromomethyl)phenyl]-2,1,3-benzothiadiazole (20): Phosphorus tribromide (160 μL, 1.72 mmol) was added dropwise at room temperature under an argon atmosphere to a solution of **19** (150 mg, 232 mmol) in dry THF (50 mL). After the mixture was stirred at room temperature for 16 h, the reaction mixture was poured into ice-water. The precipitates were collected by filtration, washed with ethanol, and purified by recrystallization from chloroform to give **20** (90 mg, 0.19 mmol, 44%) as green needles. M.p. 282–284 °C; ^{1}H NMR (270 MHz, $CDCl_3$, 25 °C, TMS): $\delta=4.60$ (s, 4H; CH_2), 7.58 (d, $J=8.6$ Hz, 4H; CH_2), 7.80 (s, 2H; ArH), 7.97 ppm (d, $J=8.6$ Hz, 4H; ArH); IR (KBr): $\tilde{\nu}=1481$, 1421, 1228, 1208, 1104, 889, 838 cm^{-1}; elemental analysis calcd (%) for $C_{20}H_{14}Br_2N_2S$ (474.2): C 50.66, H 2.98, N 5.91; found: C 50.54, H 2.94, N 5.79.

4,7-Bis[4-(dimethoxyphosphorylmethyl)phenyl]-2,1,3-benzothiadiazole (21): Trimethyl phosphite (146 mg, 1.18 mmol) and **20** (140 mg, 0.29 mmol) were heated at 160 °C for 12 h. The excess trimethyl phosphite was removed by distillation. The residue was purified by silica gel column chromatography (KANTO 60N) eluting with chloroform/methanol 18:1 to give **21** (110 mg, 0.21 mmol, 71%) as a green powder. M.p. 135–136 °C; ^{1}H NMR (270 MHz, $CDCl_3$, 25 °C, TMS): $\delta=3.27$ (d, $J=21.8$ Hz, 4H; CH_2), 3.74 (d, $J=10.8$ Hz, 12H; OCH_3), 7.49 (dd, $J=2.3$, 8.3 Hz, 4H; ArH), 7.86 (s, 2H; ArH), 7.95 ppm (d, $J=8.3$ Hz, 4H; ArH); IR (KBr): $\tilde{\nu}=1517$, 1476, 1425, 1249 (P=O), 1186, 858 cm^{-1}; FAB-MS (NBA): m/z: 532 $[M^+]$; elemental analysis calcd (%) for $C_{24}H_{26}N_2O_6P_2S$ (532.4): C 54.13, H 4.92, N 5.26; found: C 54.04, H 4.92, N 5.21.

4-[(*N*,*N*-Diphenylamino)phenyl]-7-(4-hydroxymethylphenyl)-2,1,3-benzothiadiazole (24): Sodium tetrahydroborate (35 mg, 0.93 mmol) was added to a solution of **23** (150 mg, 0.31 mmol) in ethanol (20 mL). The mixture was heated at 80 °C for 1 h, cooled to room temperature, and poured into water (60 mL). The precipitates were collected by filtration, washed with hexane, and purified by recrystallization from chloroform/hexane to give **24** (140 mg, 0.29 mmol, 93%) as a red powder. M.p. 203–204 °C; ^{1}H NMR (270 MHz, $CDCl_3$, 25 °C, TMS): $\delta=1.69$ (t, $J=5.6$ Hz, 1H; OH), 4.81 (d, $J=5.6$ Hz, 2H; CH_2), 7.07 (t, $J=7.3$ Hz, 2H; ArH), 7.17–7.34 (m, 10H; ArH), 7.56 (d, $J=8.1$ Hz, 2H; ArH), 7.76 (d, $J=7.6$ Hz, 1H; ArH), 7.79 (d, $J=7.6$ Hz, 1H; ArH), 7.88 (d, $J=8.7$ Hz, 2H; ArH), 7.97 ppm (d, $J=8.1$ Hz, 2H; ArH); IR (KBr): $\tilde{\nu}=3427$ (OH), 1590, 1486, 1324, 1283, 1195, 1179, 890, 818 cm^{-1}; FAB-MS (NBA): m/z: 485 $[M^+]$; elemental analysis calcd (%) for $C_{31}H_{23}N_3OS\cdot0.03\,CHCl_3$ (489.2): C 76.18, H 4.75, N 8.59; found: C 76.15, H 4.80, N 8.62.

4-[4-(Bromomethyl)phenyl]-7-[4-(*N*,*N*-diphenylamino)phenyl]-2,1,3-benzothiadiazole (25): Phosphorus tribromide (10 μL, 0.10 mmol) was added dropwise at 0 °C under an argon atmosphere to a solution of **24** (100 mg, 0.21 mmol) in dry THF (20 mL). After the mixture was stirred at room temperature for 3 h, the reaction mixture was poured into ice-water and extracted with toluene (50 mL × 3). The combined organic layers were dried over anhydrous magnesium sulfate and evaporated in vacuo to dryness. The residue was purified by silica gel column chromatography (KANTO 60N) eluting with chloroform/hexane 1:1 and recrystallized from chloroform/hexane to give **25** (62 mg, 0.11 mmol, 53%) as red needles. M.p. 186–188 °C; ^{1}H NMR (270 MHz, $CDCl_3$, 25 °C, TMS): $\delta=4.59$ (s, 2H; CH_2), 7.07 (t, $J=7.3$ Hz, 2H; ArH), 7.18–7.34 (m, 10H; ArH), 7.58 (d, $J=8.3$ Hz, 2H; ArH), 7.76 (d, $J=7.6$ Hz, 1H; ArH), 7.79 (d, $J=7.6$ Hz, 1H; ArH), 7.89 (d, $J=8.7$ Hz, 2H; ArH), 7.97 ppm (d, $J=8.3$ Hz, 2H; ArH); IR (KBr): $\tilde{\nu}=1589$, 1481, 1318, 1279, 887, 823, 752 cm^{-1}; FAB-MS (NBA): m/z: 547, 549 $[M+H^+]$; elemental analysis calcd (%) for $C_{31}H_{22}BrN_3S$ (548.5): C 67.88, H 4.04, N 7.66; found: C 67.99, H 4.02, N 7.62.

4-[4-(Dimethoxyphosphorylmethyl)phenyl]-7-[4-(*N*,*N*-diphenylamino)-phenyl]-2,1,3-benzothiadiazole (26): Trimethyl phosphite (285 mg, 2.35 mmol) and **25** (130 mg, 0.24 mmol) were heated at 150 °C for 12 h. The reaction mixture was poured into hexane (150 mL) after cooling. The precipitates were collected by filtration and washed well with hexane to give **26** (115 mg, 0.20 mmol, 83%) as orange prisms. M.p. 198–201 °C; ^{1}H NMR (270 MHz, $CDCl_3$, 25 °C, TMS): $\delta=3.27$ (d, $J=21.8$ Hz, 2H; CH_2), 3.74 (d, $J=10.9$ Hz, 6H; OCH_3), 7.07 (t, $J=7.3$ Hz, 2H; ArH), 7.17–7.33 (m, 10H; ArH), 7.48 (dd, $J=2.6$, 8.3 Hz, 2H; ArH), 7.75 (d, $J=7.9$ Hz, 1H; ArH), 7.78 (d, $J=7.9$ Hz, 1H; ArH), 7.88 (d, $J=8.3$ Hz, 2H; ArH), 7.95 ppm (d, $J=7.6$ Hz, 2H, ArH); IR (KBr): $\tilde{\nu}=1590$, 1483 (P=O), 1329, 1282, 1248, 1180, 1055, 1027, 888, 861, 830 cm^{-1}; FAB-MS (NBA): m/z: 577 $[M^+]$; elemental analysis calcd (%) for $C_{33}H_{28}N_3O_3PS$ (577.6): C 68.62, H 4.89, N 7.29; found: C 68.68, H 4.91, N 7.27.

X-ray Structural determinations: X-ray crystallography was performed on a Rigaku RAXIS RAPID imaging plate diffractometer with graphite

monochromated $Mo_{K\alpha}$ radiation ($\lambda = 0.71070$ Å). The data were collected at 123 K by using ω scan in the θ range of 3.3–30.0° (**1c**) and 3.0–27.6° (**7**). Data collection and cell refinement were done by using MSC/AFC Diffractometer Control (Rigaku). The structures were solved by direct method (SIR97) and were refined using full-matrix least squares (CRYSTALS) based on F^2 of all independent reflections measured. All H atoms were located at ideal positions. They were included in the refinement, but restricted to riding on the atom to which they were bonded. Isotropic thermal factors of H atoms were held to 1.2 to 1.5 times U_{eq} of the riding atoms. For more information see Table 6.

Table 6. Crystallographic data for **1c** and **7**.

	1c	**7**
formula	$C_{42}H_{30}N_4S$	$C_{18}H_{12}N_2S$
M	622.79	288.37
T [K]	123	123
crystal system	triclinic	triclinic
space group	$P\bar{1}$ (no. 2)	$P\bar{1}$ (no. 2)
a [Å]	7.6837(9)	9.597(7)
b [Å]	9.991(1)	12.05(1)
c [Å]	20.947(2)	13.959(9)
α [°]	88.602(4)	109.74(6)
β [°]	89.112(7)	94.27(7)
γ [°]	86.523(5)	111.99(6)
V [Å^3]	1604.5(1)	1371(1)
Z	2	4
ρ_{calcd} [g cm^{-1}]	1.289	1.397
μ [mm^{-1}]	0.139	0.229
$F(000)$	652	600
crystal size [mm^3]	$0.35\times0.30\times0.10$	$0.40\times0.10\times0.03$
θ range [°]	3.3–30.0	3.0–27.6
index range	$-10\le h\le 10$	$-12\le h\le 12$
	$-14\le k\le 13$	$-13\le k\le 15$
	$-29\le l\le 28$	$-18\le l\le 17$
reflections collected	76820	54140
reflections unique	9312	6221
R_{int}	0.049	0.064
data [$F^2 > 2\sigma(F^2)$]	6312	3579
parameters	455	404
goodness-of-fit	1.000	1.033
$R1/wR^2$ [$F^2 > 2\sigma(F^2)$]	0.067/0.160	0.043/0.070
$R1/wR^2$ (all data)	0.094/0.200	0.087/0.075
resd. min/max [e Å^{-3}]	−0.48/0.89	−0.63/0.60

CCDC-244164 (**1c**) and -244163 (**7**) contain the supplementary crystallographic data for this paper. These data can be obtained free of charge via www.ccdc.cam.ac.uk/conts/retrieving.html.

Two-photon absorption measurement: Two-photon absorption cross-sections at 800 nm were measured by using an open aperture Z scan method with femtosecond pulses which were generated from an 1 kHz repetition Ti/sapphire regenerative amplifier system (Quantronix Integra). The pulse width is 120 fs and the spatial profiles were characterized by knife-edge method and can be a Gaussian profile. The experimental setup for open aperture Z scan measurements is schematically shown in Figure 11. Excitation wavelength dependence of TPA cross-sections was measured using output pulses from an optical parametric amplifier (Quantronix TOPAS), where an output from the Integra system was used as a light source. Other measurement setup is almost same as the setup at 800 nm except for optical filters. The laser beam was split into two parts. One of them was monitored by a Si P-I-N photodetector (MODEL 818-SL, New Focus) as an intensity reference and the rest was used for the transmittance measurement. After passing through an $f=50$ cm lens, the laser beam was focused and passed through a quartz cell filled with the solution sample. The position of the sample cell could be varied along the laser-beam direction (z axis), so the local power density within the sample cell could be changed under a constant laser power level. The laser power level was controlled at about a 10 mW by inserting ND filters and the power density was changed from 1–50 GW cm^{-2}. The thickness of the cell is 1 cm. The transmitted laser beam from the sample cell was then detected by same type of the photo-detector as used for reference monitoring. Same measurements were done for a cell filled with the solvent alone. The transmittance can be acquired by dividing the solution-transmitted intensity by the solvent-transmitted intensity.

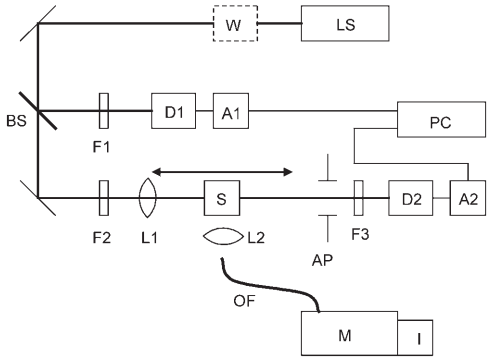

Figure 11. Experimental setup for two-photon absorption cross-section measurement: LS, light source; W, OPA wavelength converter; BS, beam splitter; F1, F2, F3, ND filters and color filters; L1, L2, lens; S, sample cell; D1, D2, detector; AP, open aperture; A1, A2, amplifier; PC, personal computer; OF, optical fiber; M, monochromator; I, I-CCD detector.

The excitation power dependence of the transmittance was analyzed by the following method.[52] The beam intensity change along the propagation direction (z axis) can be described as

$$dI/dz + \alpha I + \beta I^2 = 0 \quad (1)$$

where α is the attenuation coefficient that is due to linear absorption and scattering, and β is the nonlinear absorption coefficient that is due to TPA. Within the approximation of small linear absorption, that is, $\alpha z \ll 1$, the result of Equation (1) is:

$$I(z) = \{I(0)\exp(-\alpha z)\}/\{1 + \beta z I(0)\} \quad (2)$$

and the transmittance of the nonlinear medium can be written as

$$T(z) = I(z)/I(0) = \exp(-\alpha z)/\{1 + \beta z I(0)\} = T_0/\{1 + \beta z I(0)\} = T_0 T_i \quad (3)$$

where $I(0)$ is the initial intensity, T_0 is the linear transmittance independent of $I(0)$ and T_i is the nonlinear transmittance dependent on $I(0)$. If the spatial beam profile can be assumed as Gaussian, the nonlinear transmittance T_i should be rewritten as[53]

$$T_i = \{\ln(1 + I_0 L\beta)\}/I_0 L\beta \quad (4)$$

By fitting the experimental nonlinear transmittance data T_i with Equation (4), one can determine the nonlinear absorption coefficient β for a given input intensity $I(0)=I_0$ and a given sample thickness $z=L$. After obtaining the nonlinear absorption coefficient β, the TPA cross-section σ of one solute molecule (in units of cm^{4}s per photon) can be determined by using the following relationship:

$$\beta = \{\sigma N_A d \times 10^{-3}\}/h\nu \quad (5)$$

where N_A is the Avogadro constant, d is the concentration of the TPA compound in the solution (in units of mol L^{-1}), h is the Planck constant, and ν is the frequency of incident laser. The experimental uncertainty of σ value amounts to ±12%.

[1] M. Göppert-Mayer, *Ann. Phys.* **1931**, *9*, 273–294.
[2] a) G. S. He, J. D. Bhawalkar, C. F. Zhao, P. N. Prasad, *Appl. Phys. Lett.* **1995**, *67*, 2433–2435; b) G. S. He, G. C. Xu, P. N. Prasad, B. A. Reinhardt, J. C. Bhatt, A. G. Dillard, *Opt. Lett.* **1995**, *20*, 435–437; c) J. E. Ehrlich, X. L. Wu, I.-Y. S. Lee, Z.-Y. Hu, H. Röckel, S. R. Marder, J. W. Perry, *Opt. Lett.* **1997**, *22*, 1843–1845; d) G. S. He, T.-C. Lin, P. N. Prasad, C.-C. Cho, L.-J. Yu, *Appl. Phys. Lett.* **2003**, *82*, 4717–4719; e) H. Lei, H. Z. Wang, Z. C. Wei, X. J. Tang, L. Z. Wu, C. H. Tung, G. Y. Zhou, *Chem. Phys. Lett.* **2001**, *333*, 387–390.
[3] a) S. Maruo, O. Nakamura, S. Kawata, *Opt. Lett.* **1997**, *22*, 132–134; b) S. Kawata, H.-B. Sun, T. Tanaka, K. Takada, *Nature* **2001**, *412*, 697–698; c) W. Zhou, S. M. Kuebler, K. L. Braun, T. Yu, J. K. Cammack, C. K. Ober, J. W. Perry, S. R. Marder, *Science* **2002**, *296*, 1106–1109; d) Y. Lu, F. Hasegawa, T. Goto, S. Ohkuma, S. Fukuhara, Y. Kawazu, K. Totani, T. Yamashita, T. Watanabe, *J. Mater. Chem.* **2004**, *14*, 75–80.
[4] a) D. A. Parthenopoulos, P. M. Rentzepis, *Science* **1989**, *245*, 843–845; b) B. H. Cumpston, S. P. Ananthavel, S. Barlow, D. L. Dyer, J. E. Ehrlich, L. L. Erskine, A. A. Heikal, S. M. Kuebler, I.-Y. S. Lee, D. McCord-Maughon, J. Qin, H. Röckel, M. Rumi, X.-L. Wu, S. R. Marder, J. W. Perry, *Nature* **1999**, *398*, 51–54; c) K. D. Belfield, K. J. Schafer, *Chem. Mater.* **2002**, *14*, 3656–3662; d) K. D. Belfield, Y. Liu, R. A. Negres, M. Fan, G. Pan, D. J. Hagan, F. E. Hernandez, *Chem. Mater.* **2002**, *14*, 3663–3667.
[5] a) P. K. Frederiksen, M. Jørgensen, P. R. Ogilby, *J. Am. Chem. Soc.* **2001**, *123*, 1215–1221; b) T. D. Poulsen, P. K. Frederiksen, M. Jørgensen, K. V. Mikkelsen, P. R. Ogilby, *J. Phys. Chem. A* **2001**, *105*, 11488–11495; c) W. R. Dichtel, J. M. Serin, C. Edder, J. M. J. Fréchet, M. Matuszewski, L.-S. Tan, T. Y. Ohulchanskyy, P. N. Prasad, *J. Am. Chem. Soc.* **2004**, *126*, 5380–5381; d) M. Drobizhev, Y. Stepanenko, Y. Dzenis, A. Karotki, A. Rebane, P. N. Taylor, H. L. Anderson, *J. Am. Chem. Soc.* **2004**, *126*, 15352–15353; e) P. K. Frederiksen, S. P. McIlroy, C. B. Nielsen, L. Nikolajsen, E. Skovsen, M. Jørgensen, K. V. Mikkelsen, P. R. Ogilby, *J. Am. Chem. Soc.* **2005**, *127*, 255–269; f) M. Drobizhev, Y. Stepanenko, Y. Dzenis, A. Karotki, A. Rebane, P. N. Taylor, H. L. Anderson, *J. Phys. Chem. B* **2005**, *109*, 7223–7236; g) M. A. Oar, J. M. Serin, W. R. Dichtel, J. M. J. Fréchet, T. Y. Ohulchanskyy, P. N. Prasad, *Chem. Mater.* **2005**, *17*, 2267–2275.
[6] a) W. Denk, J. H. Strickler, W. W. Webb, *Science* **1990**, *248*, 73–76; b) J. Mertz, C. Xu, W. W. Webb, *Opt. Lett.* **1995**, *20*, 2532–2534; c) W. Denk, K. Svoboda, *Neuron* **1997**, *18*, 351–357; d) R. H. Köhler, J. Cao, W. R. Zipfel, W. W. Webb, M. R. Hanson, *Science* **1997**, *276*, 2039–2042.
[7] a) T. Euler, P. B. Detwiler, W. Denk, *Nature* **2002**, *418*, 845–852; b) M. J. Miller, S. H. Wei, I. Parker, M. D. Cahalan, *Science* **2002**, *296*, 1869–1873; c) D. R. Larson, W. R. Zipfel, R. M. Williams, S. W. Clark, M. P. Bruchez, F. W. Wise, W. W. Webb, *Science* **2003**, *300*, 1434–1436.
[8] a) L. Ventelon, S. Charier, L. Moreaux, J. Mertz, M. Blanchard-Desce, *Angew. Chem.* **2001**, *113*, 2156–2159; *Angew. Chem. Int. Ed.* **2001**, *40*, 2098–2101; b) M. Taki, J. L. Wolford, T. V. O'Halloran, *J. Am. Chem. Soc.* **2004**, *126*, 712–713; c) H. M. Kim, M.-Y. Jeong, H. C. Ahn, S.-J. Jeon, B. R. Cho, *J. Org. Chem.* **2004**, *69*, 5749–5751; d) S. J. K. Pond, O. Tsutsumi, M. Rumi, O. Kwon, E. Zojer, J.-L. Brédas, S. R. Marder, J. W. Perry, *J. Am. Chem. Soc.* **2004**, *126*, 9291–9306; e) H. Y. Woo, J. W. Hong, B. Liu, A. Mikhailovsky, D. Korystov, G. C. Bazan, *J. Am. Chem. Soc.* **2005**, *127*, 820–821.
[9] M. Albota, D. Beljonne, J.-L. Brédas, J. E. Ehrlich, J.-Y. Fu, A. A. Heikal, S. E. Hess, T. Kogej, M. D. Levin, S. R. Marder, D. McCord-Maughon, J. W. Perry, H. Röckel, M. Rumi, G. Subramaniam, W. W. Webb, X.-L. Wu, C. Xu, *Science* **1998**, *281*, 1653–1656.
[10] E. Cogné-Laage, J.-F. Allemand, O. Ruel, J.-B. Baudin, V. Croquette, M. Blanchard-Desce, L. Jullien, *Chem. Eur. J.* **2004**, *10*, 1445–1455.
[11] N. N. P. Moonen, R. Gist, C. Boudon, J.-P. Gisselbrecht, P. Seiler, T. Kawai, A. Kishioka, M. Gross, M. Irie, F. Diederich, *Org. Biomol. Chem.* **2003**, *1*, 2032–2034.
[12] a) B. A. Reinhardt, L. L. Brott, S. J. Clarson, A. G. Dillard, J. C. Bhatt, R. Kannan, L. Yuan, G. S. He, P. N. Prasad, *Chem. Mater.* **1998**, *10*, 1863–1874; b) K. D. Belfield, D. J. Hagan, E. W. Van Stryland, K. J. Schafer, R. A. Negres, *Org. Lett.* **1999**, *1*, 1575–1578; c) K. D. Belfield, K. J. Schafer, W. Mourad, B. A. Reinhardt, *J. Org. Chem.* **2000**, *65*, 4475–4481; d) R. Kannan, G. S. He, L. Yuan, F. Xu, P. N. Prasad, A. G. Dombroskie, B. A. Reinhardt, J. W. Baur, R. A. Vaia, L.-S. Tan, *Chem. Mater.* **2001**, *13*, 1896–1904.
[13] a) Z.-Q. Liu, Q. Fang, D. Wang, G. Xue, W.-T. Yu, Z.-S. Shao, M.-H. Jiang, *Chem. Commun.* **2002**, 2900–2901; b) Z.-Q. Liu, Q. Fang, D. Wang, D.-X. Cao, G. Xue, W.-T. Yu, H. Lei, *Chem. Eur. J.* **2003**, *9*, 5074–5084; c) D.-X. Cao, Z.-Q Liu, Q. Fang, G.-B. Xu, G. Xue, G.-Q. Liu, W.-T. Yu, *J. Organomet. Chem.* **2004**, *689*, 2201–2206.
[14] D.-X. Cao, Q. Fang, D. Wang, Z.-Q. Liu, G. Xue, G.-B. Xu, W.-T. Yu, *Eur. J. Org. Chem.* **2003**, 3628–3636.
[15] J. Kawamata, M. Akiba, T. Tani, A. Harada, Y. Inagaki, *Chem. Lett.* **2004**, *33*, 448–449.
[16] A. Abbotto, L. Beverina, R. Bozio, A. Facchetti, C. Ferrante, G. A. Pagani, D. Pedron, R. Signorini, *Org. Lett.* **2002**, *4*, 1495–1498.
[17] Y. Iwase, K. Kamada, K. Ohta, K. Kondo, *J. Mater. Chem.* **2003**, *13*, 1575–1581.
[18] Z.-Q. Liu, Q. Fang, D.-X. Cao, D. Wang, G.-B. Xu, *Org. Lett.* **2004**, *6*, 2933–2936.
[19] a) L. Ventelon, L. Moreaux, J. Mertz, M. Blanchard-Desce, *Chem. Commun.* **1999**, 2055–2056; b) O. Mongin, L. Porrès, L. Moreaux, J. Mertz, M. Blanchard-Desce, *Org. Lett.* **2002**, *4*, 719–722.
[20] M. Rumi, J. E. Ehrlich, A. A. Heikal, J. W. Perry, S. Barlow, Z. Hu, D. McCord-Maughon, T. C. Parker, H. Röckel, S. Thayumanavan, S. R. Marder, D. Beljonne, J.-L. Brédas, *J. Am. Chem. Soc.* **2000**, *122*, 9500–9510.
[21] K. D. Belfield, A. R. Morales, J. M. Hales, D. J. Hagan, E. W. Van Stryland, V. M. Chapela, J. Percino, *Chem. Mater.* **2004**, *16*, 2267–2273.
[22] O. S. Pyun, W. Yang, M.-Y. Jeong, S.-H. Lee, K. M. Kang, S.-J. Jeon, B. R. Cho, *Tetrahedron Lett.* **2003**, *44*, 5179–5182.
[23] K. Ogawa, A. Ohashi, Y. Kobuke, K. Kamada, K. Ohta, *J. Am. Chem. Soc.* **2003**, *125*, 13356–13357.
[24] G. P. Bartholomew, M. Rumi, S. J. K. Pond, J. W. Perry, S. Tretiak, G. C. Bazan, *J. Am. Chem. Soc.* **2004**, *126*, 11529–11542.
[25] For multi-branched TPA molecules with a triphenylamine core, see: a) S.-J. Chung, K.-S. Kim, T.-C. Lin, G. S. He, J. Swiatkiewicz, P. N. Prasad, *J. Phys. Chem. B* **1999**, *103*, 10741–10745; b) S.-J. Chung, T.-C. Lin, K.-S. Kim, G. S. He, J. Swiatkiewicz, P. N. Prasad, G. A. Baker, F. V. Bright, *Chem. Mater.* **2001**, *13*, 4071–4076; c) J. Yoo, S. K. Yang, M.-Y. Jeong, H. C. Ahn, S.-J. Jeon, B. R. Cho, *Org. Lett.* **2003**, *5*, 645–648; d) O. Mongin, L. Porrès, C. Katan, T. Pons, J. Mertz, M. Blanchard-Desce, *Tetrahedron Lett.* **2003**, *44*, 8121–8125; e) L. Porrès, O. Mongin, C. Katan, M. Charlot, T. Pons, J. Mertz, M. Blanchard-Desce, *Org. Lett.* **2004**, *6*, 47–50; f) W. J. Yang, D. Y. Kim, C. H. Kim, M.-Y. Jeong, S. K. Lee, S.-J. Jeon, B. R. Cho, *Org. Lett.* **2004**, *6*, 1389–1392; g) H. J. Lee, J. Sohn, J. Hwang, S. Y. Park, H. Choi, M. Cha, *Chem. Mater.* **2004**, *16*, 456–465; h) M. Drobizhev, A. Karotki, A. Rebane, C. W. Spangler, *Opt. Lett.* **2001**, *26*, 1081–1083.
[26] For multi-branched TPA molecules with a tricyanobenzene core, see: a) B. R. Cho, K. H. Son, S. H. Lee, Y.-S. Song, Y.-K. Lee, S.-J. Jeon, J. H. Choi, H. Lee, M. Cho, *J. Am. Chem. Soc.* **2001**, *123*, 10039–10045; b) B. R. Cho, M. J. Piao, K. H. Son, S. H. Lee, S. J. Yoon, S.-J. Jeon, M. Cho, *Chem. Eur. J.* **2002**, *8*, 3907–3916; c) W. J. Yang, C. H. Kim, M.-Y. Jeong, S. K. Lee, M. J. Piao, S.-J. Jeon, B. R. Cho, *Chem. Mater.* **2004**, *16*, 2783–2789.
[27] For multi-branched TPA molecules with a triazine core, see: a) R. Kannan, G. S. He, T.-C. Lin, P. N. Prasad, R. A. Vaia, L.-S. Tan, *Chem. Mater.* **2004**, *16*, 185–194; b) F. M. B. Li, S. Qian, K. Chen, H. Tian, *Chem. Lett.* **2004**, *33*, 470–471; c) Y.-Z. Cui, Q. Fang. G. Xue, G.-B. Xu, L. Yin, W.-T. Yu, *Chem. Lett.* **2005**, *34*, 644–645.
[28] A. Adronov, J. M. J. Fréchet, G. S. He, K.-S. Kim, S.-J. Chung, J. Swiatkiewicz, P. N. Prasad, *Chem. Mater.* **2000**, *12*, 2838–2841.

[29] O. Mongin, J. Brunel, L. Porrès, M. Blanchard-Desce, *Tetrahedron Lett.* **2003**, *44*, 2813–2816.
[30] A. Abbotto, L. Beverina, R. Bozio, A. Facchetti, C. Ferrante, G. A. Pagani, D. Pedron, R. Signorini, *Chem. Commun.* **2003**, 2144–2145.
[31] a) A. M. McDonagh, M. G. Humphrey, M. Samoc, B. Luther-Davies, *Organometallics* **1999**, *18*, 5195–5197; b) S. K. Hurst, M. G. Humphrey, T. Isoshima, K. Wostyn, I. Asselberghs, K. Clays, A. Persoons, M. Samoc, B. Luther-Davies, *Organometallics* **2002**, *21*, 2024–2026.
[32] a) D. W. Brousmiche, J. M. Serin, J. M. J. Fréchet, G. S. He, T.-C. Lin, S.-J. Chung, P. N. Prasad, *J. Am. Chem. Soc.* **2003**, *125*, 1448–1449; b) D. W. Brousmiche, J. M. Serin, J. M. J. Fréchet, G. S. He, T.-C. Lin, S.-J. Chung, P. N. Prasad, R. Kannan, L.-S. Tan, *J. Phys. Chem. B* **2004**, *108*, 8592–8600; c) J. Qu, C. Kohl, M. Pottek, K. Müllen, *Angew. Chem.* **2004**, *116*, 1554–1557; *Angew. Chem. Int. Ed.* **2004**, *43*, 1528–1531; d) A. Margineanu, J. Hofkens, M. Cotlet, S. Habuchi, A. Stefan, J. Qu, C. Kohl, K. Müllen, J. Vercammen, Y, Engelborghs, T. Gensch, F. C. De Schryver, *J. Phys. Chem. B* **2004**, *108*, 12242–12251; e) L.-M. Fu, X.-F. Wen, X.-C. Ai, Y. Sun, Y.-S. Wu, J.-P. Zhang, Y. Wang, *Angew. Chem.* **2005**, *117*, 757–760; *Angew. Chem. Int. Ed.* **2005**, *44*, 747–750.
[33] Previous report: S. Kato, T. Matsumoto, T. Ishi-i, T. Thiemann, M. Shigeiwa, H. Gorohmaru, S. Maeda, Y. Yamashita, S. Mataka, *Chem. Commun.* **2004**, 2342–2343, where the TPA cross-sections were measured only at 800 nm. In this work, they were more systematically measured between 700–800 nm.
[34] a) J.-M. Raimundo, P. Blanchard, H. Brisset, S. Akoudad, J. Roncali, *Chem. Commun.* **2000**, 939–940; b) M. Akhtaruzzaman, M. Tomura, M. B. Zaman, J. Nishida, Y. Yamashita, *J. Org. Chem.* **2002**, *67*, 7813–7818; c) M. J. Edelmann, J.-M. Raimundo, N. F. Utesch, F. Diederich, C. Boudon, J.-P. Gisselbrecht, M. Gross, *Helv. Chim. Acta* **2002**, *85*, 2195–2213.
[35] K. R. J. Thomas, J. T. Lin, M. Velusamy, Y.-T. Tao, C.-H. Chuen, *Adv. Funct. Mater.* **2004**, *14*, 83–90.
[36] a) C. Kitamura, S. Tanaka, Y. Yamashita, *Chem. Mater.* **1996**, *8*, 570–578; b) H. A. M. van Mullekom, J. A. J. M. Vekemans, E. W. Meijer, *Chem. Eur. J.* **1998**, *4*, 1235–1243; c) C. G. Bangcuyo, U. Evans, M. L. Myrick, U. H. F. Bunz, *Macromolecules* **2001**, *34*, 7592–7594; d) Y.-H. Niu, J. Huang, Y. Cao, *Adv. Mater.* **2003**, *15*, 807–811.
[37] X. Zhang, H. Gorohmaru, M. Kadowaki, T. Kobayashi, T. Ishi-i, T. Thiemann, S. Mataka, *J. Mater. Chem.* **2004**, *14*, 1901–1904.
[38] A. S. D. Sandanayaka, K. Matsukawa, T. Ishi-i, S. Mataka, Y. Araki, O. Ito, *J. Phys. Chem. B* **2004**, *108*, 19995–20004.
[39] The red shift is not attributed to the aggregation under the high concentration. The UV/Vis spectra scarcely changed at the concentration of 10^{-3}–10^{-5} M.
[40] K. Kamada, K. Ohta, Y. Iwase, K. Kondo, *Chem. Phys. Lett.* **2003**, *372*, 386–393.
[41] W. J. Yang, D. Y. Kim, M.-Y. Jeong, H. M. Kim, Y. K. Lee, X. Fang, S.-J. Jeon, B. R. Cho, *Chem. Eur. J.* **2005**, *11*, 4191–4198.
[42] P. P. Ghoroghchian, P. R. Frail, K. Susumu, D. Blessington, A. K. Brannan, F. S. Bates, B. Chance, D. A. Hammer, M. J. Therien, *Proc. Natl. Acad. Sci. USA* **2005**, *102*, 2922–2927.
[43] R. Weissleder, V. Ntziachristos, *Nat. Med.* **2003**, *9*, 123–128.
[44] K. Pilgram, M. Zupan, R. Skiles, *J. Heterocycl. Chem.* **1970**, *7*, 629–633.
[45] B. E. Koene, D. E. Loy, M. E. Thompson, *Chem. Mater.* **1998**, *10*, 2235–2250.
[46] a) K.-T Wong, Y.-Y. Chien, Y.-L. Liao, C.-C. Lin, M.-Y. Chou, M.-K. Leung, *J. Org. Chem.* **2002**, *67*, 1041–1044; b) M.-K. Leung, M.-Y. Chou, Y. O. Su, C. L. Chiang, H.-L. Chen, C. F. Yang, C.-C. Yang, C.-C. Lin, H.-T. Chen, *Org. Lett.* **2003**, *5*, 839–842.
[47] T. Ishi-i, T. Hirayama, K. Murakami, H. Tashiro, T. Thiemann, K. Kubo, A. Mori, S. Yamasaki, T. Akao, A. Tsuboyama, T. Mukaide, K. Ueno, S. Mataka, *Langmuir* **2005**, *21*, 1261–1268.
[48] Z. H. Li, M. S. Wong, Y. Tao, M. D'Iorio, *J. Org. Chem.* **2004**, *69*, 921–927.
[49] G. N. Tew, M. U. Pralle, S. I. Stupp, *Angew. Chem.* **2000**, *112*, 527–531; *Angew. Chem. Int. Ed.* **2000**, *39*, 517–521.
[50] T. Grawe, T. Schrader, M Gurrath, A. Kraft, F. Osterod, *Org. Lett.* **2000**, *2*, 29–32.
[51] H. J. Lee, J. Sohn, J. Hwang, S. Y. Park, *Chem. Mater.* **2004**, *16*, 456–465.
[52] G. S. He, L. Yuan, N. Cheng, J. D. Bhawalkar, P. N. Prasad, L. L. Brott, S. J. Clarson, B. A. Reinhardt, *J. Opt. Soc. Am. B* **1997**, *14*, 1079–1087.
[53] L. W. Tutt, T. F. Boggess, *Prog. Quantum Electron*, **1993**, *17*, 299–338.

Received: July 30, 2005
Published online: December 19, 2005

